

Marine and terrestrial nitrifying bacteria are sources of diverse bacteriohopanepolyols

Felix J. Elling^{1,*}, Thomas W. Evans², Vinitra Nathan¹, Jordon D. Hemingway¹, Jenan J. Kharbush^{1,3}, Barbara Bayer⁴, Eva Spieck⁵, Fatima Husain², Roger E. Summons², Ann Pearson¹

¹Department of Earth and Planetary Sciences, Harvard University, Cambridge, MA 02138, USA

²Department of Earth, Atmospheric, and Planetary Sciences, Massachusetts Institute of Technology, Cambridge, MA 02139, USA

³University of Michigan, Department of Earth and Environmental Science, Ann Arbor, MI 48109

⁴Department of Ecology, Evolution and Marine Biology, University of California, Santa Barbara, CA, USA

⁵Department of Microbiology and Biotechnology, University of Hamburg, 22609 Hamburg, Germany

*Corresponding author: felix_elling@fas.harvard.edu

Acknowledgements

All data are available in the supplementary materials. We thank three anonymous reviewers for comments that helped improve an earlier version of this manuscript. We thank Alyson E. Santoro (University of California, Santa Barbara) for providing bacterial strains as well as Susan Carter (Harvard) and Fatima Hussain (MIT) for laboratory assistance. This work

This is the author manuscript accepted for publication and has undergone full peer review but has not been through the copyediting, typesetting, pagination and proofreading process, which may lead to differences between this version and the [Version of Record](#). Please cite this article as [doi: 10.1111/GBI.12484](https://doi.org/10.1111/GBI.12484)

was funded through National Science Foundation grants 1702262 and 1843285 and the Gordon and Betty Moore Foundation (to A.P.). T.W.E. acknowledges funding by the Alexander von Humboldt-Stiftung through the Feodor-Lynen-Fellowship. Research at MIT was otherwise supported by the NASA Exobiology Program grant number 18-EXXO18-0039. B.B. was supported by the Austrian Science Fund (FWF) project Number J4426-B. E.S. thanks the National Park Service for permission to perform research in Yellowstone National Park (Permit YELL-2007-SCI-5698).

Author Manuscript

1
2
3
4
5
6
7
8
9
10
11
12
13
14
15
16
17
18
19
20
21
22
23
24
25
26

PROF. ROGER EVERETT SUMMONS (Orcid ID : 0000-0002-7144-8537)

Article type : Original Article

Marine and terrestrial nitrifying bacteria are sources of diverse bacteriohopanepolyols

Felix J. Elling^{1,*}, Thomas W. Evans², Vinitra Nathan¹, Jordon D. Hemingway¹, Jenan J. Kharbush^{1,3}, Barbara Bayer⁴, Eva Spieck⁵, Fatima Husain², Roger E. Summons², Ann Pearson¹

¹Department of Earth and Planetary Sciences, Harvard University, Cambridge, MA 02138, USA

²Department of Earth, Atmospheric, and Planetary Sciences, Massachusetts Institute of Technology, Cambridge, MA 02139, USA

³University of Michigan, Department of Earth and Environmental Science, Ann Arbor, MI 48109

⁴Department of Ecology, Evolution and Marine Biology, University of California, Santa Barbara, CA, USA

⁵Department of Microbiology and Biotechnology, University of Hamburg, 22609 Hamburg, Germany

*Corresponding author: felix_elling@fas.harvard.edu

Abstract

Hopanoid lipids, bacteriohopanols and bacteriohopanepolyols, are membrane components exclusive to bacteria. Together with their diagenetic derivatives, they are

27 commonly used as biomarkers for specific bacterial groups or biogeochemical processes in
28 the geologic record. However, the sources of hopanoids to marine and freshwater
29 environments remain inadequately constrained. Recent marker gene studies suggest
30 widespread potential for hopanoid biosynthesis in marine bacterioplankton, including
31 nitrifying (i.e., ammonia- and nitrite-oxidizing) bacteria. To explore their hopanoid
32 biosynthetic capacities, we studied the distribution of hopanoid biosynthetic genes in the
33 genomes of cultivated and uncultivated ammonia-oxidizing (AOB), nitrite-oxidizing (NOB),
34 and complete ammonia oxidizing (comammox) bacteria, finding that biosynthesis of diverse
35 hopanoids is common among seven of the nine presently cultivated clades of nitrifying
36 bacteria. Hopanoid biosynthesis genes are also conserved among the diverse lineages of
37 bacterial nitrifiers detected in environmental metagenomes. We selected seven representative
38 NOB isolated from marine, freshwater and engineered environments for phenotypic
39 characterization. All tested NOB produced diverse types of hopanoids, with some NOB
40 producing primarily diploptene and others producing primarily bacteriohopanepolyols.
41 Relative and absolute abundances of hopanoids were distinct among the cultures and
42 dependent on growth conditions, such as oxygen- and nitrite-limitation. Several novel
43 nitrogen-containing bacteriohopanepolyols were tentatively identified, of which the so-called
44 BHP-743.6 was present in all NOB. Distinct carbon isotopic signatures of biomass,
45 hopanoids, and fatty acids in four tested NOB suggest operation of the reverse tricarboxylic
46 acid cycle in *Nitrospira* spp. and *Nitrospina gracilis* and of the Calvin-Benson-Bassham
47 cycle for carbon fixation in *Nitrobacter vulgaris* and *Nitrococcus mobilis*. We suggest that
48 the contribution of hopanoids by NOB to environmental samples could be estimated by their
49 carbon isotopic compositions. The ubiquity of nitrifying bacteria in the ocean today and the
50 antiquity of this metabolic process suggest the potential for significant contributions to the
51 geologic record of hopanoids.

52

53 **1. Introduction**

54 Hopanoids are terpenoid lipids produced by aerobic and anaerobic bacteria (Rohmer et
55 al., 1984; Fischer et al., 2005; Talbot et al., 2008) and are ubiquitous in the modern
56 environment and the geologic record (Ourisson & Albrecht, 1992). In living bacteria,
57 hopanoids are involved in membrane homeostasis (e.g., Ourisson et al., 1987; Welander et
58 al., 2009; Sáenz et al., 2012). They are commonly found as composite lipids called
59 bacteriohopanepolyols (BHPs), consisting of hopanoid hydrocarbon skeletons bearing

60 functionalized polar sidechains (Ourisson & Rohmer, 1992; Talbot et al., 2007, 2008; Rush et
61 al., 2016). Due to their characteristic distribution among bacteria and their structural
62 diversity, both within the hopanoid skeleton and the polar sidechain, hopanoids and BHPs are
63 used as biomarkers for diverse clades of bacteria or distinct ecological niches (e.g., Sáenz et
64 al., 2011; Ricci et al., 2013; Rush et al., 2016). Due to their diagenetic stability, hopanoids
65 are important biomarkers for elucidating biogeochemical and microbial evolution from the
66 early Proterozoic onwards (Brocks & Pearson, 2005; Brocks & Banfield, 2009; Briggs &
67 Summons, 2014).

68 Application of hopanoid biomarkers relies on the genotypic and phenotypic
69 characterization of their biosynthesis among extant bacteria (Newman et al., 2016). The
70 known diversity of hopanoid producers initially was constrained by analysis of bacterial
71 cultures (Rohmer et al., 1984; Talbot et al., 2008). The potential for wider taxonomic
72 diversity expanded considerably, however, through genomic and metagenomic
73 characterization of biosynthetic genes such as squalene-hopene cyclase (SHC), which
74 catalyzes the first step in hopanoid biosynthesis forming diploptene/diplopterol (Fig. 1; e.g.,
75 Fischer et al., 2005; Pearson et al., 2007; Ricci et al., 2014). Such metagenomic surveys have
76 outpaced phenotypic characterization, leaving many bacterial clades either unstudied or
77 understudied. Additionally, the biosynthetic pathways leading from diploptene/diplopterol to
78 the diverse array of BHPs remain only partially resolved (Fig. 1) and the phylogenetic
79 distribution of known biosynthetic genes has not been studied systematically.

80 Recent lipidomic and metagenomic surveys of SHC gene homologs identified nitrite-
81 oxidizing bacteria (NOB) of the genera *Nitrospina* and *Nitrospira* as potential sources of
82 BHPs in the marine water column, particularly in suboxic settings (Kharbush et al., 2013,
83 2015, 2018). NOB are a polyphyletic group of bacteria spanning six clades across four phyla.
84 NOB mediate the second step of nitrification, the oxidation of nitrite to nitrate, and show
85 environmental niche speciation (Spieck & Bock, 2005; Daims et al., 2016). NOB of the
86 genera *Nitrobacter* (Alphaproteobacteria) and *Candidatus Nitrotoga* (Betaproteobacteria) are
87 found primarily in freshwater, wastewater and soils (Spieck & Bock, 2005; Alawi et al.,
88 2007; Daims et al., 2016). NOB of the genus *Nitrospira* (phylum Nitrospirae), on the
89 contrary, inhabit both terrestrial and marine environments, including hydrothermal systems
90 (Spieck & Bock, 2005; Daims et al., 2016; Bayer et al., 2021). Moreover, some *Nitrospira*
91 spp. are capable of performing both steps of nitrification (ammonia and nitrite oxidation,
92 “comammox”; Daims et al., 2015; van Kessel et al., 2015), although this capacity appears to

93 be limited to strains occurring in freshwater and wastewater environments (Palomo et al.,
94 2018). In the modern ocean, *Nitrospira* spp., Nitrospinaceae (phylum Nitrospinae) and
95 *Nitrococcus* spp. (Gammaproteobacteria) are the predominant NOB (Mincer et al., 2007;
96 Santoro et al., 2010; Füssel et al., 2017; Pachiadaki et al., 2017); however, there also are
97 marine species of *Nitrobacter* (Ward & Carlucci, 1985; Ward et al., 1989). Finally, five NOB
98 from the phylum Chloroflexi (Ca. *Nitrocaldera robusta*, Ca. *Nitrotheca patiens*, and three
99 *Nitrolancea* strains) have previously been cultivated from terrestrial hydrothermal springs
100 and bioreactors (Sorokin et al., 2012; Spieck et al., 2020a, 2020b), but their environmental
101 distribution remains largely unconstrained. Despite the ubiquity of NOB in terrestrial and
102 marine ecosystems, their potential to produce hopanoids, including BHPs, has not been
103 systematically assessed and their imprint on the geologic record of hopanoids remains
104 unresolved.

105 Here we describe the use of BHPs as biomarkers for NOB, based on widespread
106 association of BHP production with the capacity for nitrite oxidation, and on characterization
107 of distinct distributions and carbon isotopic compositions of these compounds in seven
108 marine and non-marine species from four genera of NOB: *Nitrospina gracilis* (marine),
109 *Nitrospira marina* (marine), *Nitrococcus mobilis* (marine), *Nitrobacter vulgaris* (wastewater),
110 *Nitrospira moscoviensis* (heating system), *Nitrospira lenta* (wastewater), and *Nitrospira*
111 *defluvii* (wastewater). Through genomic analyses we demonstrate that BHP biosynthesis is
112 common in cultivated and uncultivated NOB with exception of the Ca. *Nitrotoga* and
113 *Nitrolancea* clades. We extended this genomic approach to other nitrifying bacteria and find
114 hopanoid biosynthesis to be ubiquitous among ammonia oxidizing bacteria (AOB) and
115 comammox bacteria. Coupled genomic-lipidomic-isotopic analysis of BHPs, as demonstrated
116 here, provides valuable insights into the adaptation mechanisms of NOB as well as their roles
117 in past ecosystems.

118 **2. Material and Methods**

119 2.1 Cultivation

120 2.1.1 Origin of cultures

121 The strains *N. gracilis* Nb-3/211, *N. marina* Nb-295, *N. mobilis* Nb-231, *N. vulgaris*
122 AB1, *N. moscoviensis* M-1, *N. lenta* BS10, and *N. defluvii* A17 were obtained from the
123 culture collection of Eva Spieck at the University of Hamburg. Strain *N. gracilis* Nb-211 was

124 obtained through the culture collection of Alyson Santoro at the University of California,
125 Santa Barbara. All combinations of strains and culture conditions are shown in Table 1.

126 2.1.2 Cultivation of nitrite-oxidizing bacteria for isotopic analysis

127 To generate sufficient biomass for carbon isotopic analysis, the four NOB species *N.*
128 *gracilis* Nb-3/211, *N. mobilis* Nb-231, *N. marina* Nb-295, and *N. vulgaris* AB1 were grown
129 autotrophically in 10 L glass bottles containing 6 L of medium. *N. gracilis* Nb-3/211, *N.*
130 *mobilis* Nb-231, and *N. marina* Nb-295 were grown in a natural seawater medium (Watson &
131 Waterbury, 1971; Lücker et al., 2013) using 30% ultra-pure water and 70% Gulf of Maine
132 seawater (0.2 µm sterile-filtered; Bigelow National Center for Marine Algae and Microbiota,
133 East Boothbay, ME, USA). *N. vulgaris* was grown in an artificial freshwater medium (Bock
134 et al., 1983). After autoclaving, the media were left at room temperature for 1-3 days
135 followed by pH adjustment to 7.5 using sterile-filtered 1 M NaOH or HCl. Before
136 inoculation, 0.3 mM NaNO₂ (final concentration) was added from a sterile stock solution.
137 Cultures were inoculated with 1% of mid-growth phase pre-cultures and incubated without
138 stirring at 28 °C in the dark. After consumption of 0.3 mM nitrite, the cultures were
139 continuously stirred (150 rpm). Nitrite was then fed incrementally due to sensitivity of some
140 NOB to high nitrite concentrations during early growth (Spieck & Lipski, 2011). An
141 additional 0.5 mM nitrite was added to each culture and replenished when 0.4 mM of the
142 addition was consumed; this continued until a total of 2.3 mM nitrite had been consumed,
143 after which a final increment of 5 mM nitrite was added. Growth was monitored by
144 photometric quantification of nitrite (Strickland & Parsons, 1972). Cultures were harvested in
145 early stationary phase after consumption of 7.3 mM nitrite.

146 2.1.3 Cultivation of nitrite-oxidizing bacteria for lipidomic analyses

147 To evaluate the effects of growth parameters on hopanoid composition, the seven NOB
148 *N. gracilis* Nb-3/211, *N. marina* Nb-295, *N. mobilis* Nb-231, *N. vulgaris* AB1, *N.*
149 *moscoviensis* M-1, *N. lenta* BS10, and *N. defluvii* A17 were grown with 150 mL medium in
150 250-mL Erlenmeyer flasks at 28 °C in the dark (37 °C for *N. moscoviensis*). Triplicate
151 autotrophic cultures were grown on artificial freshwater or natural seawater media as
152 described above. In addition, the influence of different growth conditions on hopanoid
153 distributions was tested, using four NOB strains (*N. gracilis* Nb-3/211, *N. marina* Nb-295, *N.*
154 *mobilis* Nb-231, *N. vulgaris* AB1). However, some experiments were limited to specific
155 strains due to distinct growth requirements (Table 1). Growth was assessed by monitoring

156 nitrite consumption or optical density at 600 nm (OD_{600}). Cultures were harvested at the
157 beginning of stationary phase, defined as the first day after unchanged OD_{600} values or nitrite
158 concentration. Mid-growth phase nitrite oxidation rates are given in Table S1.

159 *N. vulgaris* AB1 was grown in batch cultures under chemolithoautotrophic (mid growth
160 phase, early stationary phase), heterotrophic aerobic, heterotrophic anaerobic, and aerobic
161 mixotrophic conditions. To test the influence of methionine and hydroxocobalamin (vitamin
162 B12a), 7 mM $NaNO_2$ were added to the medium and either 0.5 μ M hydroxocobalamin or 0.5
163 μ M methionine were added. To additionally investigate the effect of light, autotrophic
164 cultures amended with 0.5 μ M hydroxocobalamin and 0.5 μ M methionine were grown under
165 6 h light/18 h dark cycles (fluorescent cool-white lamps). Heterotrophic aerobic cultures were
166 grown with added 1.5 g L⁻¹ yeast extract (Difco), 1.5 g L⁻¹ peptone (Difco), and 0.55 g L⁻¹
167 sodium pyruvate. Growth of aerobic heterotrophic cultures was monitored by measuring
168 OD_{600} . Heterotrophic anaerobic (nitrate-reducing) cultures were grown in heterotrophic
169 medium with 1 g L⁻¹ $NaNO_3$ in serum bottles gas-tight blue butyl rubber stoppers. Oxygen
170 was purged from the medium and headspace using an ultrasonic bath and replaced with
171 sterile N_2 . Mixotrophic cultures were grown aerobically in heterotrophic medium with 7 mM
172 $NaNO_2$ added. Growth of anaerobic heterotrophic and mixotrophic cultures was monitored by
173 quantifying nitrite formation/consumption and OD_{600} . All cultures were agitated using an
174 orbital shaker (150 rpm) during incubation.

175 *N. gracilis*, *N. marina* Nb-295 and *N. mobilis* Nb-231 were grown
176 chemolithoautotrophically in triplicate batch cultures in natural seawater medium as well as
177 with addition of either 0.5 μ M methionine or 0.5 μ M hydroxocobalamin. Additionally, *N.*
178 *marina* Nb-295 was grown under mixotrophic conditions. For mixotrophic growth, 0.15 g L⁻¹
179 peptone, 0.15 g L⁻¹ yeast extract, 0.055 g L⁻¹ sodium pyruvate, and 7 mM $NaNO_2$ were added
180 to the medium. Additional cultures of *N. marina* and *N. mobilis* grown with 0.5 μ M
181 methionine and 0.5 μ M hydroxocobalamin were harvested during late stationary phase, i.e.,
182 two weeks after nitrite depletion.

183 To investigate the ability for hopanoid methylases to use the cyanobacterial vitamin B₁₂
184 variant pseudocobalamin, *N. marina* Nb-295, *N. mobilis* Nb-231 and *N. vulgaris* AB1 were
185 grown chemolithoautotrophically in single batch cultures in artificial seawater or freshwater
186 medium containing 100 nM pseudocobalamin. As pure pseudocobalamin was not
187 commercially available, it was extracted from 4 g of commercial *Spirulina* dietary

188 supplement as described by Heal et al. (2017) and purified using Thermo Scientific HyperSep
189 C₁₈ solid phase extraction cartridges, yielding a fraction containing 1.5 µg of
190 hydroxopseudocobalamin with traces of cyanopseudocobalamin and other non-cobalamin
191 solutes. Pseudocobalamin was quantified using an Agilent 1260 Infinity series high
192 performance liquid chromatograph (HPLC) coupled to an Agilent 6410 triple-quadrupole
193 mass spectrometer (MS). The MS was operated in multiple reaction monitoring mode, to
194 monitor the parent ions and transitions of hydroxopseudocobalamin,
195 adenosylpseudocobalamin, and cyanopseudocobalamin as described in Heal et al. (2017).
196 The HPLC method was modified from Heal et al. (2017) by using a Phenomenex Kinetex C₁₈
197 column (4.6 × 150 mm; 2.6 µm particle size), a flow rate of 1 mL min⁻¹, and 90% water/10%
198 acetonitrile (v/v) as the initial solvent composition. Hydroxocobalamin, adenosylcobalamin,
199 and cyanocobalamin standards were used to optimize ionization parameters and instrument
200 performance. As no hydroxopseudocobalamin standard was available, concentrations were
201 estimated using a hydroxocobalamin solution and assuming identical instrument response.

202 2.1.4 Nitrite- and oxygen-limited continuous cultures

203 *N. vulgaris* AB1, *N. gracilis* Nb-211, and *N. mobilis* Nb-231 were additionally grown
204 in continuous culture under constant, substrate-limited conditions (chemostat). The
205 experimental setup is illustrated in Fig. S1. The chemostat consisted of a gas-tight 2.2-L
206 reactor vessel containing 2 L of culture, kept at a constant 28 °C in the dark and stirred at 150
207 rpm. For *N. vulgaris* AB1, the reactor was fed with freshwater medium containing 10 mM
208 NaNO₂, 0.5 µM hydroxocobalamin, and 0.5 µM methionine. For *N. gracilis* Nb-211, and *N.*
209 *mobilis* Nb-231, the reactor was fed with artificial seawater medium (Bayer et al., 2021)
210 containing 2 mM NaNO₂ and 0.1 µM hydroxocobalamin. For nitrite-limited growth (i.e.,
211 oxygen-replete), the cultures were constantly aerated using sterile-filtered (0.2 µm pore size),
212 humidified air delivered through aquarium pumps, resulting in full oxygen saturation (6.0 ±
213 0.2 ppm; Table S2) of the growth medium. For oxygen-limited growth (i.e., nitrite-replete),
214 aeration of the reactor was stopped, and the headspace was flushed with sterile N₂ gas (0.2
215 µm pore size filter; 0.2 L min⁻¹). The feeding medium was flushed with air to allow full
216 oxygen saturation (8.6 ± 0.2 ppm; Table S2), as the medium was the only source of dissolved
217 oxygen to the reactor. The chemostat outflow was flushed with sterile-filtered N₂ gas (0.2 L
218 min⁻¹) to inhibit growth in the collection bottle. For *N. vulgaris*, nitrite and oxygen
219 concentrations were sampled through a sterile sampling port directly from the reactor and
220 monitored continuously to assess performance of the chemostat. For *N. gracilis* Nb-211, and

221 *N. mobilis* Nb-231, samples for nitrite concentration assays were taken from the chemostat
222 outflow. Due to interference of high nitrite concentrations with the Winkler method—even
223 after the addition of sodium azide—the oxygen concentration measurements under oxygen-
224 limited conditions were considered unreliable. For all experiments, oxygen-limited conditions
225 were indicated by strongly increased nitrite concentrations in the chemostat outflow. The
226 cultures were maintained at constant growth rates (*N. mobilis* Nb-231, *N. gracilis* Nb-211:
227 0.011 h⁻¹; *N. vulgaris* AB1: 0.013 h⁻¹; Table S2, S3). Equilibrium conditions were reached
228 within 3-4 turnovers of the culture volume, as indicated by constant nitrite concentrations in
229 the reactor outflow. For all chemostat experiments, chemostat outflow was collected after
230 equilibration in a glass bottle placed in an ice bath. Cells were harvested from the outflow
231 using filtration as described below for batch cultures. For *N. vulgaris*, triplicate harvests of
232 biomass (0.2-0.6 L) were spaced apart by at least one full turnover (2-3 days) of the
233 chemostat vessel. For *N. gracilis* Nb-211 and *N. mobilis* Nb-231, biomass was sampled daily
234 (~0.5 L) and combined to yield duplicate samples of 1 L for each species and condition. Cell
235 densities were determined by epifluorescence microscopy of 2% formaldehyde-fixed samples
236 using SYBR Green I staining (Lunau et al., 2005).

237 2.1.5 Harvesting and lipid extraction

238 Biomass was harvested by filtration through two stacked, combusted glass fiber filters
239 (GF-75, 0.3 µm pore size, Advantec MFS, Dublin, CA, USA). Lipids were extracted using a
240 four-step Bligh and Dyer extraction (Bligh & Dyer, 1959) using an ultrasonic bath and as
241 modified by Sturt et al. (2004) and Sáenz (2010). The total lipid extracts (TLEs) were gently
242 dried under N₂, reconstituted in dichloromethane:methanol 5:1, and stored at -20 °C.

243 2.2 Mass-spectrometric analysis of bacteriohopanepolyols

244 BHPs in dried TLE aliquots for all experiments were acetylated with 100 µL acetic
245 anhydride and 100 µL pyridine at 50 °C for 1 h and then left overnight at room temperature
246 (Spencer-Jones, 2015). After acetylation, samples were evaporated to dryness, reconstituted
247 in 30:70 methanol/isopropanol, filtered through 0.45 µm pore size syringe-tip PTFE filters,
248 and stored at -20 °C until analysis. Aliquots of the acetylated TLEs were injected into a
249 coupled HPLC-MS system consisting of a 1200 series HPLC and a 6520 quadrupole time-of-
250 flight mass spectrometer (QTOF-MS) equipped with an atmospheric-pressure chemical
251 ionization interface operated in positive mode (all Agilent Technologies, Santa Clara, CA,
252 USA). The mass spectrometer was calibrated before analysis, with a typical error in mass

253 accuracy of < 1 ppm, and two reference masses were constantly monitored. The ion source
254 was set to the following parameters: gas temperature 325°C, vaporizer temperature 350°C, N₂
255 drying gas flow 6 L min⁻¹, N₂ nebulizer flow 40 L min⁻¹, capillary voltage 1200 V, corona
256 needle current 4 μA, and fragmentor voltage 150 V (Matys et al., 2017). Analyses were
257 performed in full-scan mode with a scan rate of 2 spectra per second over the m/z range of
258 200-1300 for MS¹ mode and 100-1300 for MS² mode. MS² precursor selection was
259 performed in data-dependent mode targeting the two most abundant ions per MS¹ scan with
260 an isolation width of 4 Da and active exclusion after 2 spectra over 0.4 min. BHPs were
261 chromatographically separated using a Poroshell 120 EC-C₁₈ column (2.1 × 150 mm, 2.7 μm
262 particle size; Agilent Technologies) following the protocol of Matys et al. (2017). BHPs were
263 identified by retention time, MS² fragment spectra, accurate molecular mass, and isotope
264 pattern match of proposed sum formulas in full scan mode using Agilent MassHunter B.06.00
265 and Bruker DataAnalysis 4.4 software. Absolute quantification was achieved by normalizing
266 hopanoid concentrations to consumed substrate (mmol NO₂⁻ oxidized). BHP concentrations
267 were corrected for differences in relative response using authentic standards of diplopterol, 2-
268 Me diplopterol, bacteriohopanetetrol (BHT), 2-Me BHT, and aminobacteriohopanetriol
269 (BHaminotriol). Due to lack of standards for some compounds, the relative response of
270 BHaminotriol was used for correction of other nitrogen-containing BHPs and the relative
271 response of 2-Me BHT was used to correct abundances of 3-Me BHT. We therefore consider
272 the reported relative abundances of BHPs to be semi-quantitative. The lower limit of
273 detection was estimated at 13 pg on-column (relative abundance of <0.01% of total
274 hopanoids), as determined by the lowest concentration of a BHP (monounsaturated BHT)
275 detected in the culture extracts. Averages and 1σ standard deviations of hopanoid relative
276 abundances and concentrations from triplicate cultures are given in Supplementary Datafile
277 S2.

278 2.3 Isotopic analysis of dissolved inorganic carbon, bacteriohopanepolyols, biomass, and 279 fatty acids

280 Isotopic analyses were performed only for chemolithoautotrophically-grown batch
281 cultures of *N. marina*, *N. gracilis*, *N. mobilis*, and *N. vulgaris* as described in section 2.1.2.
282 The primary goal of the isotopic analyses was to confirm operation of the predicted carbon
283 fixation pathways and to characterize the isotopic offsets between biomass and lipids derived
284 from the isoprenoid (hopanoids) and acetogenic (fatty acids) pathways. Headspace-free
285 samples for stable carbon isotopic composition of dissolved inorganic carbon ($\delta^{13}\text{C}_{\text{DIC}}$) were

286 collected immediately after inoculation by overflowing 30 mL glass bottles with culture and
287 capping with Qorpak polycone caps. 20 μ L of saturated HgCl₂ solution were added to inhibit
288 microbial activity and samples were stored at 4 °C in the dark. Values of $\delta^{13}\text{C}_{\text{DIC}}$ were
289 determined in triplicate at the University of Florida Light Stable Isotope Mass Spec Lab using
290 a Thermo Finnigan DeltaPlus XL isotope ratio mass spectrometer (IRMS) coupled to a
291 GasBench II interface. The long-term precision of samples and reference standard
292 measurements was < 0.1‰. All results are reported in delta notation relative to VPDB.
293 $\delta^{13}\text{C}_{\text{CO}_2}$ was calculated from $\delta^{13}\text{C}_{\text{DIC}}$ after Mook et al. (1974), at 28 °C. During growth,
294 increasing utilization of the dissolved inorganic carbon pool could have led to Rayleigh
295 fractionation, which could have affected apparent ¹³C fractionation values presented in Table
296 2. However, no significant difference in $\delta^{13}\text{C}_{\text{DIC}}$ was observed for samples collected from *N.*
297 *gracilis* cultures at three growth phases: early growth phase (0.17 ± 0.44 ‰), mid-growth
298 phase (0.36 ± 0.43 ‰), and stationary phase (-0.16 ± 0.64 ‰).

299 Biomass stable carbon isotopic composition was analyzed in triplicate using a
300 ThermoScientific Flash EA coupled to a Delta V Plus IRMS. Filter samples were freeze-
301 dried, decarbonated with 1 N HCl, and dried at 60 °C. Stable carbon isotopic compositions
302 were peak-size-corrected and offset-corrected using laboratory and authentic reference
303 standards (glutamic acid: -13.90‰ $\delta^{13}\text{C}$ VPDB; tyrosine: -24.90‰; USGS40: -26.39‰;
304 USGS41a: 36.55‰).

305 Free and intact polar lipid-bound fatty acids in the TLE were converted to fatty acid
306 methyl esters (FAMES) following the protocol of Ichihara and Fukubayashi (2010) and were
307 analyzed as described in (Tang et al., 2017). To monitor instrument performance, the fatty
308 acid standards were analyzed in between every batch of three sample analyses. Due to
309 insufficient chromatographic separation, $\delta^{13}\text{C}$ values of C₁₆ fatty acids were determined as the
310 integrated value of C_{16:0}+C_{16:1 ω 5}+C_{16:1 ω 9} fatty acids for *N. marina* and C_{16:0}+C_{16:1 ω 9} fatty acids
311 for *N. mobilis*. Similarly, $\delta^{13}\text{C}$ values of C₁₈ fatty acids were determined as the integrated
312 value of C_{18:0}+C_{18 ω 7} fatty acids for *N. mobilis* and C_{18:0}+C_{18 ω 1} fatty acids for *N. vulgaris*. The
313 $\delta^{13}\text{C}$ values were corrected for (i) size-effects using dilution series of standards (C_{16:0}, C_{19:0},
314 C_{24:0} fatty acids) of known isotopic composition and (ii) carbon derived from
315 transesterification using the same standards prepared in parallel to the samples (Tang et al.,
316 2017).

317 The $\delta^{13}\text{C}$ values of diploptene were analyzed in triplicate from TLE aliquots, using the
318 same instrumental setup and employing the corrections described above using an n-C₃₈
319 alkane standard of known isotopic composition (obtained from Arndt Schimmelmann,
320 Indiana University).

321 2.4 Homology detection and phylogenetic analysis of hopanoid and cobalamin biosynthesis 322 genes

323 Hopanoid biosynthesis gene homologs were identified through sequence homology,
324 conserved domains, and by clustering with reference sequences in phylogenetic trees.
325 Genomes of NOB were searched for hopanoid biosynthesis protein homologs using blastp
326 v2.7.1 (Altschul et al., 1990). Reference sequences (from Alicyclobacillus acidocaldarius,
327 Burkholderia cenocepacia, Burkholderia pseudomallei, Koribacter versatilis, Methylococcus
328 capsulatus, Nostoc punctiforme, Rhodospseudomonas palustris) were selected based on two
329 criteria: (i) previously identified hopanoid biosynthesis gene homologs and (ii) production of
330 the respective hopanoid confirmed through lipid analysis. Reference protein sequences were
331 obtained through the UniProt database (<http://www.uniprot.org>) and were searched against all
332 draft and finished NOB genomes in the NCBI genome database
333 (<http://www.ncbi.nlm.nih.gov/genome>), the NCBI non-redundant protein database, as well as
334 environmental metagenome-assembled genomes (MAG) and single cell amplified genomes
335 (SAG) of NOB in the Integrated Microbial Genomes & Metagenomes database of the Joint
336 Genome Institute (<http://img.jgi.doe.gov>), using an expectation value cutoff of 10^{-5} . Complete
337 and nearly complete 16S rRNA gene sequences of NOB and AOB were obtained through the
338 NCBI and SILVA databases (Quast et al., 2013) or manually retrieved from genomes. For
339 phylogenetic analyses, protein or nucleotide sequences were aligned using MAFFT v7.388
340 (Kato & Standley, 2013) in multi-domain (G-INS-i) and single-domain (L-INS-i) modes,
341 respectively, and manually refined. Maximum-likelihood phylogenies were generated using
342 RAxML v7.4.2 (Stamatakis, 2014) using gamma distribution estimates and the Whelan &
343 Goldman amino acid substitution model for proteins. Bootstrap support was calculated 500
344 times for each analysis. Phylogenetic trees were visualized using iTOL v3 (Letunic & Bork,
345 2016).

346 3. Results

347 3.1 Distribution of hopanoid biosynthetic genes in nitrifying bacteria

348 Hopanoid biosynthetic gene homologs were detected in all sequenced cultures of the
349 NOB/comammox families Nitrospiraceae and Nitrospinaceae, the genera Nitrococcus and
350 Nitrobacter, as well as the Chloroflexi NOB *Ca. Nitrotheca patiens* and *Ca. Nitrocaldera*
351 *robusta* (Fig. 2; Supplementary Datafile S1). Similarly, all sequenced genomes of cultivated
352 AOB (e.g., *Nitrosomonas europaea*, *Nitrosococcus oceani*) encoded hopanoid biosynthetic
353 genes. By contrast, no homologs were detected in the NOB genera *Ca. Nitrotoga* and
354 *Nitrolancea*. The presence of hopanoid biosynthetic genes was not conserved among some
355 closely related groups, such as in the phylum Nitrospirae, in which only two of four
356 characterized genera (*Nitrospira* and *Leptospirillum*) contained hopanoid biosynthesis gene
357 homologs. Only a subset of the studied environmental genomes (metagenome-assembled
358 genomes and single cell genomes) contained hopanoid biosynthesis gene homologs
359 (Supplementary Datafile S1). All hopanoid biosynthesis genes detected in environmental
360 genomes were also found in cultivated representatives, implying that the biosynthetic
361 capacity of the cultured species is generally representative for uncultured species of nitrifying
362 bacteria.

363 Most NOB and AOB representatives that contain a putative gene for the initial step of
364 hopanoid biosynthesis, the formation of diploptene/diplopterol by the enzyme squalene
365 hopene cyclase (SHC; Sohlenkamp & Geiger, 2016; Belin et al., 2018), also contain *hpnH*
366 and *hpnG* homologs. These genes encode enzymes for the biosynthesis of the
367 polyfunctionalized hopanoids adenosylhopane and ribosylhopane, respectively (Bradley et
368 al., 2010; Welander et al., 2012; Liu et al., 2014; Sato et al., 2020). Gene homologs for
369 biosynthetic steps downstream of ribosylhopane and leading to the formation of N-
370 acetylglucosaminyl BHT (*hpnI*), BHT cyclitol ether (*hpnJ*), and glucosaminyl BHT (*hpnK*)
371 (Schmerk et al., 2015), were detected in only two AOB (*Ca. Nitrosoglobus terrae* and *Ca.*
372 *Nitrosacidococcus tergens*). In addition, a single NOB (*Ca. N. robusta*) contained *hpnK* but
373 not *hpnI* and *hpnJ*. The gene coding for the biosynthesis of BHaminotriol from ribosylhopane
374 (*hpnO*) (Welander et al., 2012) was detected in *Nitrococcus* and *Nitrobacter* spp. as well as
375 all betaproteobacterial AOB (*Nitrosomonas*, *Nitrosovibrio*, *Nitrosospira*), but not in the
376 gammaproteobacterial AOB (*Nitrosococcus*, *Ca. Nitrosoglobus*, *Ca. Nitrosacidococcus*).
377 Homologs of *hpnO* could not be unequivocally identified in *Nitrospira* spp., as multiple
378 homologous amino acid aminotransferases were detected. However, these homologs shared
379 low sequence similarity ($\leq 30\%$) and did not cluster with any previously identified *hpnO*
380 homologs in phylogenetic trees.

381 Homologs coding for hopanoid A-ring methylases were found in almost all
382 NOB/comammox and some AOB. Homologs of the hopanoid C-2 methylase hpnP (Welander
383 et al., 2010) were found only in *Nitrobacter* spp. and a single *Nitrospira* sp., *Ca. Nitrospira*
384 *alkalitolerans* (Fig. 2). By contrast, homologs coding for the C-3 methylase, hpnR (Welander
385 & Summons, 2012), were more widespread and found in *N. mobilis*, all *Nitrosococcus* spp.
386 and all *Nitrospira* spp. except for *N. defluvii* and *N. lenta* (Fig. 2).

387 3.2 Distribution of hopanoids in chemolithoautotrophically-grown nitrite-oxidizing bacteria

388 As a baseline experiment, we characterized hopanoid production in
389 chemolithoautotrophic cultures. The seven studied NOB produced a diverse suite of 25
390 BHPs. Six novel BHPs with the ions of 762.5, 656.5, 771.6, 748.5, 638.5, and 743.6 Da were
391 tentatively identified using MS² spectra and molecular formulas derived from accurate
392 masses (Fig. 3; Table S4; interpretation of fragmentation patterns is provided in the
393 supplementary information). Major BHPs common to all strains were adenosylhopane, BHT,
394 BHaminotriol, and the novel BHP-743.6 and BHP-762.5, with minor amounts of other BHPs
395 (Fig. 4 & 5; Supplementary Datafile S2).

396 Although each NOB produced a similar array of BHPs, their relative abundances were
397 variable (Fig. 4 & 5). Each of the three non-marine *Nitrospira* spp. contained a different
398 major BHP: adenosylhopane in *N. defluvii* (56%), BHP-743.6 in *N. lenta* (55%), and BHT in
399 *N. moscoviensis* (54%). 35-Aminobacteriohopanepentol (BHaminopentol) was detected in
400 significant amounts (4%) only in *N. defluvii*. *N. marina* contained predominantly BHT.
401 Analysis of one additional large-volume culture (8 L) allowed detection of additional minor
402 BHPs in *N. marina*—C₁₆, C₁₈, and C₁₉ n-acylaminotriol BHPs that were not detected in any
403 other NOB species. No methylated BHPs were detected in *N. marina*. The most abundant
404 BHPs in *N. gracilis* were BHT (74%), BHP-743.6 (18%), and BHaminotriol (8%; Fig. 5). No
405 methylated BHPs were detected in *N. gracilis*. In contrast, BHP-743.6 (45%) and
406 BHaminotriol (44%) were the most abundant BHPs in *N. mobilis*, with minor contributions
407 from BHT (2%) and other BHPs, including methylcarbamate triol (7%). *N. mobilis* contained
408 trace amounts of 3-Me BHT (0.04%) but no other forms of 3-Me BHPs. *N. vulgaris*
409 contained BHaminotriol (50%), BHP-743.6 (29%), adenosylhopane (9%), and BHT (2%).
410 2-Me BHT was detected in trace amounts in *N. vulgaris* (<0.1%) but no other forms of 2-Me
411 BHPs were found in cultures grown chemolithoautotrophically (Fig. 4).

412 The non-functionalized hopanoid diploptene was present in all cultures (Fig. 4 & 5).
413 Diploptene comprised 99% of total hopanoids (BHPs + diploptene) in *N. marina*, whereas
414 lower abundances were found in *N. lenta* (89%), *N. moscoviensis* (78%), *N. gracilis* (69%),
415 *N. vulgaris* (37%), and *N. defluvii* (11%). Diploptene was detected only in trace amounts in
416 *N. mobilis*. Trace amounts (0.5%) of 2-Me diploptene were detected in *N. vulgaris*, and 3-Me
417 diploptene was not detected in any strain under these conditions.

418 3.3 Effects of changes in culturing conditions on hopanoid distributions in nitrite-oxidizing 419 bacteria

420 Changes in growth conditions (Table 1) had no effect on hopanoid distribution in
421 batch cultures of *N. marina* and *N. mobilis* (Fig. 5), except for late stationary phase cultures,
422 where lower amounts of methylcarbamate triol were observed in *N. mobilis* and slightly
423 lower amounts of BHT and higher amounts of BHaminotriol were detected in *N. marina*.
424 Trace amounts of 3-methyl diploptene were observed in cultures of *N. marina* supplemented
425 with cobalamin. Chemostat cultures of *N. mobilis* grown under NO_2^- or O_2 -limited conditions
426 had broadly similar hopanoid distributions. By contrast, BHP compositions of *N. gracilis* and
427 *N. vulgaris* changed notably with growth conditions. In *N. gracilis*, cultures supplemented
428 with methionine and cobalamin resulted in an increase of the BHP to diploptene ratio and
429 higher abundance of minor BHPs (Fig. 5). *N. gracilis* grown under NO_2^- -limited conditions
430 produced predominantly diploptene (~95%) over BHPs but this ratio was reversed under O_2 -
431 limitation (~94% BHPs). Similarly, *N. vulgaris* cultures supplemented with cobalamin
432 produced more BHPs relative to diploptene, as well as more 2-Me-BHPs, 2-Me-diploptene,
433 and BHaminotriol relative to the other BHPs (Fig. 4; Elling et al., 2020). These changes were
434 also observed for *N. vulgaris* grown mixotrophically, heterotrophically (anaerobic), and when
435 grown under NO_2^-/O_2 -limited conditions in chemostats. Under heterotrophic aerobic
436 conditions, *N. vulgaris* showed lower relative abundance of total BHPs but the highest 2-Me-
437 BHP abundance of any tested condition. Under mixotrophic conditions and autotrophic
438 conditions with added pseudocobalamin, *N. vulgaris* produced higher amounts of
439 BHaminopentol (15% and 6%, respectively) compared to all other growth conditions (<2%).
440 Finally, autotrophic cultures of *N. vulgaris* grown without cobalamin and methionine and
441 harvested in mid-growth phase contained >90% adenosylhopane (Fig. 4).

442 3.4 Changes in hopanoid concentrations in nitrite-oxidizing bacteria

443 Total hopanoid concentrations were normalized to substrate utilization (mmol NO₂⁻
444 oxidized) in lieu of cell counts, which enables comparison across species and between batch
445 and chemostat experiments. This approach circumvents biases caused by varying cell size but
446 also reflects the different energy requirements of the different carbon fixation pathways
447 employed by NOB. Total hopanoid concentrations varied strongly across growth conditions
448 and between species (Fig. 4 & 5). During chemolithoautotrophic growth, the highest
449 concentrations were observed in *N. vulgaris* and *N. marina* (27 µg/mmol NO₂⁻) and the
450 lowest concentrations were observed in *N. moscoviensis* (0.01 µg/mmol NO₂⁻).

451 3.5 Carbon isotopic composition of biomass, fatty acids, and hopanoids in nitrite-oxidizing 452 bacteria

453 The biomass of all four tested, chemolithoautotrophically-grown NOB was depleted in
454 ¹³C relative to CO₂, with *N. vulgaris* showing a more pronounced fractionation ($\epsilon_{\text{CO}_2\text{-biomass}} =$
455 $23.2 \pm 0.3\text{‰}$) compared to *N. mobilis* ($8.5 \pm 0.3\text{‰}$), *N. gracilis* ($2.0 \pm 0.3\text{‰}$), and *N. marina*
456 ($1.8 \pm 0.1\text{‰}$; Table 2). Carbon isotopic compositions of fatty acids showed strong ¹³C-
457 depletion relative to CO₂ in *N. mobilis* ($\epsilon_{\text{CO}_2\text{-C}_{16}\text{FA}} = 16.6 \pm 0.1\text{‰}$, $\epsilon_{\text{CO}_2\text{-C}_{18}\text{FA}} = 13.8 \pm 0.6\text{‰}$)
458 and *N. vulgaris* ($\epsilon_{\text{CO}_2\text{-C}_{18}\text{FA}} = 30.1 \pm 0.3\text{‰}$). Fractionation relative to CO₂ was small in *N.*
459 *gracilis* ($\epsilon_{\text{CO}_2\text{-C}_{16}\text{FA}} = -0.4 \pm 0.3\text{‰}$) and *N. marina* ($\epsilon_{\text{CO}_2\text{-C}_{16}\text{FA}} = -3.5 \pm 0.4\text{‰}$). The hopanoid
460 diploptene showed greater carbon isotopic fractionation relative to CO₂ ($\epsilon_{\text{CO}_2\text{-diploptene}}$)
461 compared to biomass and fatty acids in *N. gracilis* ($7.4 \pm 0.9\text{‰}$), *N. marina* ($7.1 \pm 0.2\text{‰}$), and
462 *N. vulgaris* ($31.9 \pm 0.4\text{‰}$). The $\epsilon_{\text{CO}_2\text{-diploptene}}$ value was similar to those of the fatty acids in *N.*
463 *mobilis* ($11.7 \pm 1.7\text{‰}$). C₁₈ fatty acids were depleted relative to biomass ($\epsilon_{\text{bio-C}_{18}\text{FA}}$) in all
464 strains (Table 2). In contrast, C₁₆ fatty acids ($\epsilon_{\text{bio-C}_{16}\text{FA}}$) were depleted relative to biomass in
465 *N. mobilis* ($7.8 \pm 0.3\text{‰}$) but enriched in *N. gracilis* ($-2.4 \pm 0.3\text{‰}$) and *N. marina* ($-5.3 \pm$
466 0.4‰).

467 4. Discussion

468 4.1 Phenotypic and genotypic characterization of hopanoid production in nitrifying bacteria

469 To assess the hopanoid biosynthetic capacity of nitrifying bacteria, we surveyed the
470 genomes of ammonia-oxidizing bacteria, comammox, and nitrite-oxidizing bacteria, and
471 found that most cultivated nitrifying bacteria should be able to produce C₃₀ hopanoids (e.g.,
472 diploptene, diplopterol; encoded by the SHC gene) and side-chain extended hopanoids
473 (BHPs; Fig. 2). Similarly, 29 out of 84 surveyed incomplete environmental genomes and
474 enrichment cultures of Nitrospirae, Nitrospinae, and Nitrobacter spp. possess at least one

475 hopanoid biosynthetic gene (Supplementary Datafile S1). Among nitrifying bacteria,
476 hopanoid biosynthetic pathways are absent only in the genera *Ca. Nitrotoga*
477 (*Betaproteobacteria*) and the *Chloroflexi* NOB (*Nitrolancea*, *Ca. Nitrotheca patiens*, and *Ca.*
478 *Nitrocaldera*). Although only two complete genomes for *Ca. Nitrotoga* and none for
479 *Chloroflexi* NOB are currently available (Kitzinger et al., 2018; Ishii et al., 2020), hopanoid
480 biosynthesis genes are also absent from five near-complete *Ca. Nitrotoga* genomes and six
481 near-complete *Chloroflexi* NOB genomes (Supplementary Datafile S1; Sorokin et al., 2012;
482 Boddicker & Mosier, 2018; Spieck et al., 2020a, 2020b). This suggests that *Ca. Nitrotoga*
483 and *Chloroflexi* NOB likely do not produce hopanoids.

484 The occurrence of hopanoid biosynthetic genes may allow prediction of the types of
485 hopanoids produced by nitrifying bacteria (Bradley et al., 2010; Welander et al., 2010, 2012;
486 Welander & Summons, 2012; Liu et al., 2014; Schmerk et al., 2015). Our analyses show
487 good agreement between genomic predictions and observations in culture. All seven NOB
488 species investigated here, as well as the previously studied NOB species *Nitrospira defluvii*
489 (Lücker et al., 2010) and the AOB *Nitrosomonas europaea* (Seemann et al., 1999) contained
490 the SHC gene and produced at least C₃₀ hopanoids (Fig. 2). Similarly, *hpnG* and *hpnH* gene
491 homologs were present in most SHC-positive nitrifier genomes, and their products
492 adenosylhopane and ribosylhopane/ribonylhopane also were detected in all seven tested NOB
493 strains (Fig. 4 & 5, Supplementary Datafile S2). However, ribosylhopane, ribonylhopane, and
494 adenosylhopane were present only in small amounts in the seven NOB (with exception of *N.*
495 *defluvii*). In contrast, adenosylhopane was abundant in *N. vulgaris* in mid-growth phase
496 (>90%) and early stationary phase (up to 40%). The low abundance of these BHPs under
497 most conditions, with high abundance during mid-growth phase, likely reflects their role as
498 central intermediates in the biosynthesis of downstream BHPs (Bradley et al., 2010;
499 Welander et al., 2012; Bodlenner et al., 2015). Consequently, downstream BHPs such as
500 BHT and BHaminotriol were the most abundant BHPs in the studied NOB strains.

501 While the enzyme responsible for BHT formation remains to be identified, biosynthesis
502 of BHaminotriol is known to be facilitated by the aminotransferase *HpnO* using
503 ribonylhopane or ribosylhopane as the precursor (Welander et al., 2012). The *hpnO* gene is
504 found in NOB of the genera *Nitrobacter* and *Nitrococcus* as well as many AOB. Exceptions
505 are *gammaproteobacterial* AOB (*Nitrosococcus* spp., *Ca. Nitrosoglobus terrae*, *Ca.*
506 *Nitrosacidococcus tergens*), and several *Nitrosovibrio* and *Nitrosomonas* species.
507 BHaminotriol was observed previously in the AOB *Nitrosomonas europaea* (Seemann et al.,

1999), which contains the *hpnO* gene. Surprisingly, we did not find *hpnO* homologs in any of the closed or incomplete *Nitrospira* genomes or in the ~99% complete genome of *N. gracilis*, even though the tested species contained abundant BHaminotriol (Fig. 5). We hypothesize that BHaminotriol is produced by a different aminotransferase in these species and that absence of *hpnO* can thus not be used to infer the absence of BHaminotriol production. Downstream of BHT, the *hpnI*, *hpnJ*, and *hpnK* genes encode biosynthesis of N-acetylglucosaminyl BHT, glucosaminyl BHT, and BHT cyclitol ether (Schmerk et al., 2015). The whole pathway consisting of *hpnI*, *hpnJ*, and *hpnK* is present in only two nitrifying bacteria, the AOB *Ca. Nitrosoglobus terrae* and *Ca. Nitrosacidococcus tergens*. None of the respective BHPs were detected in the seven tested NOB. However, we identified a *hpnK* homologue in the incomplete MAG of the thermophilic Chloroflexi NOB *Ca. N. robusta*, which lacks all other hopanoid biosynthetic genes. Although this homologue could represent contamination of the MAG, no indication of contamination was found (based on contig length, position on the contig, phylogeny of neighboring genes, tetranucleotide frequency, GC content) suggesting that the rest of the biosynthetic pathway may not have been recovered during sequencing and/or assembly. Based on these results, biosynthesis of acetylglucosaminyl, glucosaminyl, and cyclitol BHTs seems to be rare among nitrifying bacteria. Schmerk et al. (2015) previously demonstrated that these BHPs enhance tolerance to low pH in *Burkholderia cenocepacia*. Likewise, cyclitol BHTs and their diagenetic derivatives are abundant in modern and ancient acidic peats (Talbot et al., 2016b, 2016a). As the *hpnIJK* genes occur only in the acid-tolerant AOB *Ca. N. terrae* (Hayatsu et al., 2017) and *Ca. N. tergens* (Picone et al., 2020) but not in neutrophilic AOB, it appears likely that the respective BHPs are involved in acclimatization to low pH.

Hopanoids can be further modified by methylation at C-2 and C-3 of the A ring, mediated by the *HpnP* and *HpnR* enzymes, respectively (Welander et al., 2010; Welander & Summons, 2012). Among nitrifying bacteria, the *hpnP* gene is common only in *Nitrobacter* species and consequently, 2-methylhopanoids were detected in *N. vulgaris*. The only other nitrifier carrying *hpnP* is *Ca. Nitrospira alkalitolerans*, an alkalitolerant freshwater NOB. The *hpnP* sequence of *Ca. N. alkalitolerans* falls into a cluster shared only with *Nitrospirae* and *Verrucomicrobia* sequences from metagenomes. The *hpnR* gene is found in both AOB (*Nitrosococcus* spp.) and NOB (*N. mobilis* and most *Nitrospira* species) and trace amounts of 3-methylhopanoids were detected in *N. mobilis* and *N. marina*. Absence of *hpnR* homologs in some *Nitrospira* spp. could result from incomplete coverage of the draft genome sequences.

541 Presence of both hpnR and hpnP in *Ca. N. alkalitolerans* (Fig. S2) suggests a capacity to
542 produce hopanoids methylated at both C-2 and C-3, which has so far only been reported from
543 the acidobacterium *Ca. Koribacter versatilis* (Sinninghe Damsté et al., 2017).

544 While the major hopanoids found in the investigated NOB were congruent with
545 predictions based on genotypes, the cultures also contained a wide range of other minor
546 hopanoids, such as BHaminopentol, bacteriohopanepentol, and methylcarbamate triol, as well
547 as novel BHPs. The biosynthetic pathways for these and other BHPs found in environmental
548 samples remain unknown. Given the abundance of amino-BHPs in the tested NOB cultures,
549 we hypothesize that HpnO and related aminotransferases could promiscuously aminate a
550 range of precursors in addition to ribonylhopane, leading to the formation of a wide range of
551 BHPs with terminal amino groups such as aminotetrol, aminopentol, aminohexol and the
552 novel compounds BHP-743.6 and BHP-771.6, as discussed in the next section.

553 There seems to be no specific pattern linking nitrification to a specific repertoire of
554 hopanoid biosynthetic genes or to similar abundances of specific hopanoids. This is possibly
555 related to the polyphyly of nitrifiers, as their repertoire of hopanoid biosynthesis genes does
556 not seem to universally follow phylogeny. For example, while all *Nitrobacter* spp. share the
557 same repertoire of hopanoid biosynthesis genes including the hpnP gene, the hpnR gene is
558 present in some but not all *Nitrospira* species. Similarly, hopanoid biosynthetic capacity
559 differs between the two studied genera of the phylum Nitrospirae, *Nitrospira* and
560 *Leptospirillum* (Fig. 2). Further, each studied *Nitrospira* species contained a different
561 dominant BHP (Fig. 4 & 5). Therefore, we conclude that hopanoid biosynthetic capacity and
562 its expression are not necessarily governed by either the primary metabolism or phylogeny
563 but could also reflect other factors such as adaptations to specific habitats and environmental
564 conditions, as suggested earlier (e.g., Doughty et al., 2009; Ricci et al., 2014).

565 4.2 Biosynthesis and physiological significance of novel BHPs in nitrite-oxidizing bacteria

566 We tentatively identified several novel nitrogen-containing BHPs in nitrite-oxidizing
567 bacteria (Fig. 3). Two of these novel BHPs putatively contained two amino groups (BHP-
568 771.6 and BHP-743.6). BHP-771.6 apparently contains one amino group connected to the C₅
569 sidechain backbone and another as part of an aminopropyl group bound to the sidechain
570 backbone via an ether bond. The incorporation of aminopropanol is unprecedented for BHPs,
571 but it is a common metabolite in bacteria, known to be involved, for instance, in the
572 biosynthesis of cobalamin (Warren et al., 2002). BHP-743.6 contains one amino group and

573 one methylamino group, both directly bound to the backbone of the sidechain. We speculate
574 that these amino groups could be derived from either a novel aminotransferase or via
575 sequential amination by a single aminotransferase, followed by methylation. No additional
576 candidate aminotransferases were detected other than HpnO within the cluster of hopanoid
577 biosynthesis genes in *N. vulgaris*. This suggests that HpnO could mediate sequential
578 amination to form BHP-743.6 from a ribonylhopane precursor. Other candidates include a
579 large number of aminotransferases outside the hopanoid biosynthetic gene cluster of *N.*
580 *vulgaris*. The scattered distribution of hopanoid biosynthetic genes in the other NOB
581 complicates the identification of candidate genes. For BHP-656.5, the structural similarity to
582 BHaminoTriol suggests that it could be derived from this compound through an unknown
583 cyclase.

584 The occurrence of two presumably nitrated BHPs (BHP-762.5 and BHP-748.5; Fig. 3)
585 is unprecedented, and their biosynthetic origin is elusive. Comparison with fatty acids offers
586 clues regarding the origin and function of nitrated BHPs. Nitro-fatty acids are common in
587 eukaryotes, where they are involved in oxidative stress response, post-translational
588 modification of proteins, and cell signaling (Schopfer & Khoo, 2019). Nitrated fatty acids are
589 thought to be formed through reaction of unsaturated fatty acids with reactive nitrogen
590 species such as $\cdot\text{NO}$, $\cdot\text{NO}_2$, and ONOO^- (Schopfer & Khoo, 2019). Analogously, reactive
591 nitrogen species formed during nitrite oxidation or assimilatory nitrate reduction could react
592 with unsaturated BHPs to form nitrated BHPs. Further research is needed to determine
593 whether nitrated BHPs are inadvertent byproducts of oxidative stress and/or whether they
594 serve physiological functions.

595 4.3 Factors influencing hopanoid distributions in nitrite-oxidizing bacteria

596 Due to the role of hopanoids in membrane organization and fluidity, bacteria adapt their
597 hopanoid composition in response to growth phases and environmental stresses (e.g.,
598 Welander et al., 2009, 2012; Sáenz et al., 2012; Wu et al., 2015; Bradley et al., 2017). Here,
599 we specifically explored the effects of metabolism (autotrophy, mixotrophy, heterotrophy,
600 NO_2^- and O_2 limitation, light) and the co-factors cobalamin (vitamin B_{12}) and methionine on
601 the production of hopanoids. Cobalamin and methionine are presumably involved in several
602 steps of hopanoid biosynthesis. Methionine and cobalamin are cofactors for the methylases
603 HpnP and HpnR (Welander et al., 2010; Welander & Summons, 2012), and methionine is a
604 predicted co-factor for the biosynthesis of BHT cyclitol ether, which is mediated by HpnJ

605 (Welander et al., 2012). Because the tested NOB do not contain *hpnJ* gene homologs, we
606 expected no production of cyclitol ethers. However, four of the seven tested NOB cannot
607 synthesize cobalamin and of these non-producers, only two can synthesize methionine in the
608 absence of cobalamin (Table S5). Therefore, we hypothesized that addition of cobalamin
609 could influence abundances of methylhopanoids.

610 The *hpnP*-encoding strain *N. vulgaris* contained only trace amounts of 2-
611 methylhopanoids (predominantly 2-methyl diploptene) when grown autotrophically on a
612 defined mineral medium without cobalamin (Fig. 4; Elling et al., 2020). Addition of
613 cobalamin to the mineral medium or growth on complex medium (containing yeast extract as
614 a cobalamin source) resulted in up to 32% of 2-methylhopanoids relative to total hopanoids.
615 Further modification of growth conditions of cobalamin-replete cultures, such as
616 heterotrophic growth or nitrite- or oxygen-limitation, resulted in comparatively small changes
617 in 2-methylhopanoid abundance. These results imply that 2-methylhopanoid abundance in *N.*
618 *vulgaris* is primarily dependent on “true” cobalamin availability and only secondarily
619 dependent on the tested growth conditions. Supplementation with pseudocobalamin—the
620 form of vitamin B₁₂ produced by cyanobacteria and likely used as co-factor by their HpnP—
621 only slightly stimulated 2-methylhopanoid production in *N. vulgaris*. We suggest that this
622 lack of 2-methylhopanoid production is caused by co-factor specificity of HpnP, potentially
623 resulting from substitutions in the cobalamin-binding domains of alphaproteobacterial versus
624 cyanobacterial HpnP (Fig. S3). Specifically, this result further supports the notion that
625 ammonia-oxidizing archaea are the most likely source of cobalamin to NOB, rather than
626 cyanobacteria (Doxey et al., 2015; Heal et al., 2017; Elling et al., 2020).

627 In the *hpnR*-encoding NOB, *N. mobilis* and *N. marina*, 3-methylhopanoids were found
628 only in trace amounts when grown on a natural seawater medium that contains only trace
629 levels of cobalamin. Addition of cobalamin, pseudocobalamin (only tested for *N. mobilis*), or
630 methionine, or mixotrophic growth on complex organics (which supply methionine and
631 cobalamin) did not stimulate production of 3-methylhopanoids (Fig. 5). Similarly, 3-
632 methylhopanoids were not detected in the cobalamin-prototroph *N. moscoviensis*. Previously,
633 Welander et al. (2012) suggested that starvation could trigger production of 3-
634 methylhopanoids, based on accumulation of 3-methylhopanoids and increased survival
635 during late stationary phase in wild-type versus *hpnR* deletion mutants of *Methylococcus*
636 *capsulatus*. Still, cultures of *N. marina* and *N. mobilis* harvested in late stationary phase two
637 weeks after nitrite consumption did not contain increased quantities of 3-methylhopanoids.

638 Thus, 3-methylhopanoid production in NOB is dependent on factors that remain to be
639 identified.

640 Variations in the composition and concentration of other BHPs in response to growth
641 conditions seem to be species-specific. For instance, *N. gracilis* produced almost exclusively
642 BHPs (94% of total hopanoids, i.e., BHPs plus diploptene and 2-methyl diploptene) when
643 grown under oxygen-limited conditions compared to nitrite-limited growth (5% BHPs), but
644 this was not observed in *N. mobilis* or *N. vulgaris* (Fig. 4 & 5). Higher abundance of BHPs
645 under oxygen-limited conditions in *N. gracilis* could be related to the upregulation of HpnH
646 (mediating the first step in BHP biosynthesis from diploptene), which was observed during
647 oxygen-limited growth of *N. marina* (Bayer et al., 2021). It has been suggested that BHPs
648 and diploptene have contrasting effects on membrane physiology, with BHPs integrating into
649 the membrane perpendicular to the membrane surface, resulting in enhanced membrane lipid
650 ordering, and diploptene localizing to the hydrophobic midplane of the lipid bilayer and
651 reducing membrane permeability (Poger & Mark, 2013; Caron et al., 2014; Mangiarotti et al.,
652 2019). This hopanoid-mediated regulation of membrane physiology appears to be less
653 important under oxygen-limited conditions. Total hopanoid concentrations were lowest under
654 oxygen-limited conditions for both *N. mobilis* and *N. gracilis*; similar changes were not
655 observed in *N. vulgaris*. A causal link between hopanoid abundance and microaerobic
656 conditions may be a higher efficiency of carbon fixation under oxygen-limitation, a
657 mechanism that may also extend to other NOB such as *Nitrospira* spp. The carbon fixation
658 pathways in *N. gracilis* and *N. mobilis*—the rTCA and the CBB cycle, respectively—contain
659 oxygen-sensitive enzymes (Erb, 2011). A significantly higher cell yield ($p < 0.05$, two-tailed
660 t-test) was observed for oxygen-limited growth over nitrite-limited growth in *N. gracilis* and
661 *N. mobilis* (Table S3). Hopanoids, and in particular diploptene, could thus serve as
662 modulators of membrane O_2 permeability in *N. mobilis* and *N. gracilis*, as previously
663 suggested for nitrogen-fixing bacteria (Berry et al., 1993). A role of hopanoids in controlling
664 oxygen permeability is a plausible explanation for both higher relative abundance of BHPs
665 over diploptene in *N. gracilis* and lower total hopanoid concentrations under oxygen-limited
666 conditions in *N. gracilis* and *N. mobilis*. Differences in BHP over diploptene abundance in
667 *N. gracilis* and *N. mobilis* as well as lack of a similar response in hopanoid composition in
668 *N. vulgaris* (cell yield was not determined), which also uses the CBB cycle, suggests distinct
669 regulation mechanisms across NOB clades. Still, our results imply that changes in

670 biogeochemical parameters such as oxygenation could significantly alter the hopanoid signal
671 in environmental samples and the geological record.

672 4.4 Hopanoids as biomarkers for nitrifying bacteria and implications for past environments

673 The sources of hopanoids in modern and past environments remain inadequately
674 characterized, especially for the marine realm. Our results confirm previous suggestions that
675 Nitrospinae and Nitrospirae may contribute to hopanoid production in the ocean (Kharbush et
676 al., 2013, 2018; Mueller et al., 2020) and expand the range of producers to include most
677 terrestrial and marine nitrifying bacteria: Nitrobacter and Nitrococcus spp., all known AOB,
678 and comammox bacteria. Because concentrations of total hopanoids varied up to 10-fold
679 between growth conditions and several orders of magnitude between species, we suggest that
680 both community composition and growth conditions could modulate the relative contribution
681 of NOB to the geological record of hopanoids. The major hopanoids of nitrifying bacteria are
682 diplopterol/diploptene, adenosylhopane, BHaminotriol, and BHT. However, these hopanoids
683 are non-specific as they are produced by a wide range of bacteria and thus are ubiquitous in
684 the ocean across the oxic-anoxic continuum, in marine sediments, freshwater, and soils
685 (Wakeham et al., 2007, 2012; Zhu et al., 2011; Berndmeyer et al., 2013; Blumenberg et al.,
686 2013). Novel hopanoids such as BHP-743.6 (tentatively a methylamino aminotriol BHP)
687 could potentially serve as biomarkers specific for NOB. However, further studies are needed
688 to confirm its specificity and diagenetic stability. Anoxic conditions, such as during oceanic
689 anoxic events or in peats, and low maturity of organic matter could help preserve BHP-743.6
690 as previously shown for other BHPs (van Dongen et al., 2006; Talbot et al., 2016a). Partial
691 loss of labile functional groups such as nitro-groups may result in loss of specificity, but the
692 putative C-N-C bond could help preserve the signature functional group of BHP-743.6 even
693 if the molecule were to be partially degraded.

694 Along with common hopanoids, some nitrifying bacteria may contribute to the
695 production of widely used biomarkers, such as BHaminopentol. In soil and freshwater
696 environments, BHaminopentol has commonly been interpreted as a biomarker for aerobic
697 methanotrophic bacteria (Talbot et al., 2014; Rush et al., 2016). Production of this compound
698 by *N. vulgaris* and *Nitrospira defluvii* suggests nitrifier sources in these environments in
699 addition to methanotrophic bacteria. Although *Nitrobacter* and *Nitrospira* spp. are unlikely
700 sources of highly ¹³C-depleted hopanoids attributed to methanotrophs (Collister et al., 1992;
701 <-50‰; Thiel et al., 2003; Birgel et al., 2006), they may have contributed to deposition of

702 many records that contain less ¹³C-depleted hopanoids (~ -30 to -40‰; e.g., Talbot et al.,
703 2014) previously attributed primarily to methanotrophs. It is possible that additional
704 nitrifying bacteria not examined here may also produce BHaminopentol. Since *N. vulgaris*
705 produced high quantities of BHaminopentol only under one growth condition (mixotrophy),
706 further investigation is needed to constrain the impact on the applicability of BHaminopentol
707 as a biomarker for methanotrophs.

708 The 2- and 3-methylhopanoids found in the marine geologic record were previously
709 thought to indicate presence of planktonic nitrogen-fixing cyanobacteria and methanotrophic
710 bacteria, respectively (Summons et al., 1999; Kuypers et al., 2004; Cao et al., 2009; Kasprak
711 et al., 2015), although other sources of these compounds have been recognized (Summons et
712 al., 1999; Rashby et al., 2007; Welander et al., 2010; Welander & Summons, 2012). Based
713 on our culture experiments and bioinformatic analyses, we propose nitrifying bacteria as
714 additional sources of these compounds. Because nitrifying bacteria depend on remineralized
715 nitrogen for energy, the abundance of nitrifying bacteria and their imprint on the sedimentary
716 record of methylhopanoids would have depended on (i) overall productivity (ii) on the
717 relative flux of nitrogen through nitrification versus anaerobic nitrogen loss processes, and
718 (iii) specific environmental conditions or physiological stresses promoting methylhopanoid
719 production. On geologic timescales, these processes are controlled by nutrient cycles (Fe, P)
720 and ocean oxygenation (Van Cappellen & Ingall, 1996; Falkowski, 1998; Tyrrell, 1999). In
721 the geologic record, widespread ocean deoxygenation, for example during Cretaceous
722 Oceanic Anoxic Event 2, was associated with enhanced nitrification rates and deposition of
723 2- and 3-methylhopanoids (e.g., Kuypers et al., 2004; Naafs et al., 2019). Based on our
724 culture experiments, we hypothesize that the proliferation of nitrifying bacteria due to
725 intensified nitrification may have contributed to methylhopanoid deposition during these
726 events. Specifically, marine AOB such as *Nitrosococcus* and NOB such as *Nitrococcus* and
727 *Nitrospira* could have contributed to 3-methylhopanoid deposition, although the specific
728 conditions triggering production of 3-methyl hopanoids in these bacteria and thus their
729 imprint on sedimentary records remain to be resolved. Similarly, marine *Nitrobacter* ecotypes
730 may have contributed 2-methylhopanoids to the geological record of these events as
731 suggested previously (Elling et al., 2020). Furthermore, detection of a HpnP sequence among
732 *Nitrospira* spp. suggests that they are potential additional sources of 2-methylhopanoids.
733 Remarkably, this and related sequences are basally related to HpnP sequences from all known
734 2-methylhopanoid producers (Fig. S2), suggesting a different phylogenetic origin of HpnP

735 than previously acknowledged (i.e., outside alphaproteobacteria and cyanobacteria; Ricci et
736 al., 2014, 2015) and the existence of further undiscovered clades of 2-methylhopanoid
737 producers (Fig. S2). Importantly, contributions of nitrifying bacteria to methylhopanoid
738 deposition do not rule out contributions from cyanobacteria and methanotrophs. However,
739 since 2-methylhopanoid biosynthesis is generally absent from contemporary marine
740 cyanobacteria (Ricci et al., 2014, 2015; Elling et al., 2020), it seems plausible that 2-
741 methylhopanoid deposition during ocean anoxic events could reflect the proliferation of
742 marine *Nitrobacter* ecotypes. Although cyanobacterial contributions to the 2-methylhopanoid
743 signal cannot be excluded, we urge caution when interpreting 2-methylhopanoid deposition
744 as evidence for proliferation of nitrogen-fixing cyanobacteria.

745 An imprint of nitrifying bacteria on the marine sedimentary record of hopanoids
746 requires efficient export of these small cells from the lower euphotic zone. The export
747 mechanisms of nitrifier biomass in the ocean remain uncharacterized but export efficiency
748 may be appreciably lower than that of surface phytoplankton due to small cell size and
749 consequently lower grazing efficiency and lack of passive sinking (Boenigk et al., 2004;
750 Close et al., 2013). Nevertheless, several lines of evidence suggest that the export efficiency
751 of small cells may be higher than canonically recognized (Richardson & Jackson, 2007;
752 Close et al., 2013; Lengger et al., 2019). This is supported by the observation of archaeal
753 biomarker accumulation during anoxic events in the Plio-Pleistocene Mediterranean Sea
754 (Menzel et al., 2006; Polik et al., 2018) and during Cretaceous oceanic anoxic event 1b in the
755 Atlantic Ocean (Kuypers, 2001; Kuypers et al., 2002). Based on their shared depth habitat
756 and similar or larger cell size (Koops et al., 2006; Mincer et al., 2007; Santoro et al., 2010;
757 Spieck & Lipski, 2011), it appears likely that biomass of other nitrifying bacteria such as
758 NOB and AOB would have been exported with similar efficiency.

759 Contributions of nitrifying bacteria to hopanoid production may be identified through
760 their distinct carbon isotopic compositions, determined here for chemolithoautotrophically-
761 grown cultures (Table 2). The low carbon isotopic fractionation of lipids and biomass relative
762 to dissolved inorganic carbon found in *N. gracilis* and *N. marina* is consistent with the
763 operation of the reverse tricarboxylic acid (rTCA) cycle for carbon fixation (Preuß et al.,
764 1989; Berg et al., 2010), as previously shown for *Nitrospira defluvii* (Lücker et al., 2010).
765 Enrichment in ^{13}C in C_{16} fatty acids relative to biomass and diploptene in *N. gracilis* and *N.*
766 *marina* reflects fractionation during acetyl-CoA generation in the rTCA cycle (Sirevåg et al.,
767 1977; van der Meer et al., 1998; Williams et al., 2006). The higher fractionation observed in

768 *N. vulgaris* is indicative of the Calvin-Benson-Bassham (CBB) cycle for carbon fixation
769 (Sirevåg et al., 1977; Berg et al., 2010). Similarly, all known AOB use the CBB cycle
770 (Supplementary Datafile S1; Sakata et al., 2008; Koops & Pommerening-Röser, 2015).
771 Through mass balance, it may be possible to distinguish or quantify contributions of
772 Nitrospina and Nitrospira spp. from those of autotrophs using the CBB cycle such as
773 Nitrobacter spp., cyanobacteria, and AOB ($\epsilon_{\text{CO}_2\text{-biomass}} = 20\text{-}30\text{‰}$; Quandt et al., 1977;
774 McNevin et al., 2007). Given that Nitrospina and Nitrospira spp. are the dominant NOB in
775 most of the modern ocean (e.g., Mincer et al., 2007; Santoro et al., 2010; Pachiadaki et al.,
776 2017), a significant contribution to hopanoid deposition should be detectable through the
777 carbon isotopic composition of hopanoids in suspended particulate matter and surface
778 sediments. To similarly recognize this signature in geological samples, knowledge of the
779 dissolved inorganic carbon isotopic composition, ideally at the habitat depth of NOB, would
780 be needed. Dissolved inorganic carbon isotopic composition could be constrained through the
781 carbon isotopic composition of lipids from ammonia-oxidizing archaea living in the same
782 ecological niche and depth habitat (Elling et al., 2021).

783 Peculiar fractionation systematics indicate that *N. mobilis* uses carbon fixation
784 pathways distinct from the other tested NOB. It has previously been suggested based on
785 genomic data that *N. mobilis* uses the CBB cycle for carbon fixation (Lücker et al., 2010;
786 Füssel et al., 2017). Yet, the ^{13}C -fractionation into biomass and lipids is much smaller than
787 expected for the CBB cycle. It remains to be tested whether this fractionation pattern results
788 from specific growth conditions or novel mechanisms of carbon fixation in *N. mobilis*.

789 **5. Conclusions**

790 The detection of hopanoids in nitrifying bacteria expands the known diversity of
791 hopanoid producers and further ties hopanoid production to the nitrogen cycle. Specifically,
792 potential for production of 2- and 3-methylhopanoids by NOB and AOB suggests that source
793 assignments of these biomarkers in geological records and modern environments need to be
794 broadened, although the specific conditions under which production of methylhopanoids is
795 stimulated in NOB (and by extension, AOB) remain unclear. Due to the ubiquity of nitrifying
796 bacteria in terrestrial, freshwater, brackish, and marine environments, it appears likely that
797 they contributed to the geologic record of hopanoids, especially in times of intensified marine
798 nitrogen cycling such as during oceanic anoxic events. The novel nitrogen-containing BHPs
799 tentatively identified here could potentially serve as biomarkers for nitrite-oxidizing bacteria.
800 Their physiological role remains elusive but a potential involvement in regulation of cellular

801 processes such as oxidative stress response, alternative respiratory pathways, and protein
802 modification warrants further attention. Further experiments on the effect of additional
803 growth conditions (e.g., temperature, pH, salinity) on hopanoid distributions as well as
804 analyses of AOB and currently uncultivated clades of NOB are needed to comprehensively
805 assess the potential of hopanoids as biomarkers for nitrifying bacteria in the geologic past.

806 **Acknowledgements**

807 We thank three anonymous reviewers for comments that helped improve an earlier
808 version of this manuscript. We thank Alyson E. Santoro (University of California, Santa
809 Barbara) for providing bacterial strains as well as Susan Carter (Harvard University) for
810 laboratory assistance. This work was funded through National Science Foundation grants
811 1702262 and 1843285 and the Gordon and Betty Moore Foundation (to A.P.). T.W.E.
812 acknowledges funding by the Alexander von Humboldt-Stiftung through the Feodor-Lynen-
813 Fellowship. Research at MIT was otherwise supported by the NASA Exobiology Program
814 grant number 18-EXXO18-0039. B.B. was supported by the Austrian Science Fund (FWF)
815 project Number J4426-B. E.S. thanks the National Park Service for permission to perform
816 research in Yellowstone National Park (Permit YELL-2007-SCI-5698).

817 **References**

- 818 Alawi M, Lipski A, Sanders T, Pfeiffer EM, Spieck E (2007) Cultivation of a novel cold-
819 adapted nitrite oxidizing betaproteobacterium from the Siberian Arctic. *The ISME Journal* **1**,
820 256–264.
- 821 Altschul SF, Gish W, Miller W, Myers EW, Lipman DJ (1990) Basic local alignment search
822 tool. *Journal of Molecular Biology* **215**, 403–410.
- 823 Bayer B, Saito MA, McIlvin MR, Lückner S, Moran DM, Lankiewicz TS, Dupont CL,
824 Santoro AE (2021) Metabolic versatility of the nitrite-oxidizing bacterium *Nitrospira marina*
825 and its proteomic response to oxygen-limited conditions. *The ISME Journal* **15**, 1025–1039.
- 826 Belin BJ, Busset N, Giraud E, Molinaro A, Silipo A, Newman DK (2018) Hopanoid lipids:
827 from membranes to plant–bacteria interactions. *Nature Reviews Microbiology* **16**, 304–315.
- 828 Berg IA, Kockelkorn D, Ramos-Vera WH, Say RF, Zarzycki J, Hügler M, Alber BE, Fuchs
829 G (2010) Autotrophic carbon fixation in archaea. *Nature Reviews Microbiology* **8**, 447–460.
- 830 Berndmeyer C, Thiel V, Schmale O, Blumenberg M (2013) Biomarkers for aerobic
831 methanotrophy in the water column of the stratified Gotland Deep (Baltic Sea). *Organic*
832 *Geochemistry* **55**, 103–111.

833 Berry AM, Harriott OT, Moreau RA, Osman SF, Benson DR, Jones AD (1993) Hopanoid
834 lipids compose the Frankia vesicle envelope, presumptive barrier of oxygen diffusion to
835 nitrogenase. *Proceedings of the National Academy of Sciences* **90**, 6091–6094.

836 Birgel D, Peckmann J, Klautzsch S, Thiel V, Reitner J (2006) Anaerobic and Aerobic
837 Oxidation of Methane at Late Cretaceous Seeps in the Western Interior Seaway, USA.
838 *Geomicrobiology Journal* **23**, 565–577.

839 Bligh EG, Dyer WJ (1959) A Rapid Method of Total Lipid Extraction and Purification.
840 *Biochemistry and Cell Biology* **37**, 911–917.

841 Blumenberg M, Berndmeyer C, Moros M, Muschalla M, Schmale O, Thiel V (2013)
842 Bacteriohopanepolyols record stratification, nitrogen fixation and other biogeochemical
843 perturbations in Holocene sediments of the central Baltic Sea. *Biogeosciences* **10**, 2725–
844 2735.

845 Bock E, Sundermeyer-Klinger H, Stackebrandt E (1983) New facultative lithoautotrophic
846 nitrite-oxidizing bacteria. *Archives of Microbiology* **136**, 281–284.

847 Boddicker AM, Mosier AC (2018) Genomic profiling of four cultivated Candidatus
848 Nitrotoga spp. predicts broad metabolic potential and environmental distribution. *The ISME*
849 *Journal* **12**, 2864–2882.

850 Bodlenner A, Liu W, Hirsch G, Schaeffer P, Blumenberg M, Lendt R, Tritsch D, Michaelis
851 W, Rohmer M (2015) C₃₅ Hopanoid Side Chain Biosynthesis: Reduction of Ribosylhopane
852 into Bacteriohopanetetrol by a Cell-Free System Derived from *Methylobacterium*
853 *organophilum*. *ChemBioChem* **16**, 1764–1770.

854 Boenigk J, Stadler P, Wiedlroither A, Hahn MW (2004) Strain-Specific Differences in the
855 Grazing Sensitivities of Closely Related Ultramicrobacteria Affiliated with the
856 Polynucleobacter Cluster. *Applied and Environmental Microbiology* **70**, 5787–5793.

857 Bradley AS, Pearson A, Sáenz JP, Marx CJ (2010) Adenosylhopane: The first intermediate in
858 hopanoid side chain biosynthesis. *Organic Geochemistry* **41**, 1075–1081.

859 Bradley AS, Swanson PK, Muller EEL, Bringel F, Carroll SM, Pearson A, Vuilleumier S,
860 Marx CJ (2017) Hopanoid-free *Methylobacterium extorquens* DM4 overproduces carotenoids
861 and has widespread growth impairment. *PLOS ONE* **12**, e0173323.

862 Briggs DEG, Summons RE (2014) Ancient biomolecules: Their origins, fossilization, and
863 role in revealing the history of life. *BioEssays* **36**, 482–490.

864 Brocks JJ, Banfield J (2009) Unravelling ancient microbial history with community
865 proteogenomics and lipid geochemistry. *Nature reviews. Microbiology* **7**, 601–609.

866 Brocks JJ, Pearson A (2005) Building the Biomarker Tree of Life. *Reviews in Mineralogy*
867 *and Geochemistry* **59**, 233–258.

868 Cao C, Love GD, Hays LE, Wang W, Shen S, Summons RE (2009) Biogeochemical
869 evidence for euxinic oceans and ecological disturbance presaging the end-Permian mass
870 extinction event. *Earth and Planetary Science Letters* **281**, 188–201.

871 Caron B, Mark AE, Poger D (2014) Some Like It Hot: The Effect of Sterols and Hopanoids
872 on Lipid Ordering at High Temperature. *The Journal of Physical Chemistry Letters* **5**, 3953–
873 3957.

874 Close HG, Shah SR, Ingalls AE, Diefendorf AF, Brodie EL, Hansman RL, Freeman KH,
875 Aluwihare LI, Pearson A (2013) Export of submicron particulate organic matter to
876 mesopelagic depth in an oligotrophic gyre. *Proceedings of the National Academy of Sciences*
877 **110**, 12565–12570.

878 Collister JW, Summons RE, Lichtfouse E, Hayes JM (1992) An isotopic biogeochemical
879 study of the Green River oil shale. *Organic Geochemistry* **19**, 265–276.

880 Daims H, Lebedeva E V., Pjevac P, Han P, Herbold C, Albertsen M, Jehmlich N, Palatinszky
881 M, Vierheilig J, Bulaev A, Kirkegaard RH, Bergen M Von, Rattei T, Bendinger B, Nielsen
882 PH, Wagner M (2015) Complete nitrification by *Nitrospira* bacteria. *Nature* **528**, 504–509.

883 Daims H, Lückner S, Wagner M (2016) A New Perspective on Microbes Formerly Known as
884 Nitrite-Oxidizing Bacteria. *Trends in Microbiology* **24**, 699–712.

885 Dongen BE van, Talbot HM, Schouten S, Pearson PN, Pancost RD (2006) Well preserved
886 Palaeogene and Cretaceous biomarkers from the Kilwa area, Tanzania. *Organic*
887 *Geochemistry* **37**, 539–557.

888 Doughty DM, Hunter RC, Summons RE, Newman DK (2009) 2-Methylhopanoids are
889 maximally produced in akinetes of *Nostoc punctiforme*: geobiological implications.
890 *Geobiology* **7**, 524–532.

891 Doxey AC, Kurtz DA, Lynch MD, Sauder LA, Neufeld JD (2015) Aquatic metagenomes
892 implicate *Thaumarchaeota* in global cobalamin production. *The ISME Journal* **9**, 461–471.

893 Elling FJ, Hemingway JD, Evans TW, Kharbush JJ, Spieck E, Summons RE, Pearson A
894 (2020) Vitamin B₁₂-dependent biosynthesis ties amplified 2-methylhopanoid production
895 during oceanic anoxic events to nitrification. *Proceedings of the National Academy of*
896 *Sciences* **117**, 32996–33004.

897 Elling FJ, Hemingway JD, Kharbush JJ, Becker KW, Polik CA, Pearson A (2021) Linking
898 diatom-diazotroph symbioses to nitrogen cycle perturbations and deep-water anoxia: Insights
899 from Mediterranean sapropel events. *Earth and Planetary Science Letters* **571**, 117110.

900 Erb TJ (2011) Carboxylases in Natural and Synthetic Microbial Pathways. *Applied and*
901 *Environmental Microbiology* **77**, 8466–8477.

902 Falkowski PG (1998) Biogeochemical Controls and Feedbacks on Ocean Primary
903 Production. *Science* **281**, 200–206.

904 Fischer WW, Summons RE, Pearson A (2005) Targeted genomic detection of biosynthetic
905 pathways: anaerobic production of hopanoid biomarkers by a common sedimentary microbe.
906 *Geobiology* **3**, 33–40.

907 Füssel J, Lücker S, Yilmaz P, Nowka B, Kessel MAHJ van, Bourceau P, Hach PF, Littmann
908 S, Berg J, Spieck E, Daims H, Kuypers MMM, Lam P (2017) Adaptability as the key to
909 success for the ubiquitous marine nitrite oxidizer *Nitrococcus*. *Science Advances* **3**,
910 e1700807.

911 Hayatsu M, Tago K, Uchiyama I, Toyoda A, Wang Y, Shimomura Y, Okubo T, Kurisu F,
912 Hirono Y, Nonaka K, Akiyama H, Itoh T, Takami H (2017) An acid-tolerant ammonia-
913 oxidizing γ -proteobacterium from soil. *The ISME Journal* **11**, 1130–1141.

914 Heal KR, Qin W, Ribalet F, Bertagnolli AD, Coyote-Maestas W, Hmelo LR, Moffett JW,
915 Devol AH, Armbrust EV, Stahl DA, Ingalls AE (2017) Two distinct pools of B₁₂ analogs
916 reveal community interdependencies in the ocean. *Proceedings of the National Academy of*
917 *Sciences* **114**, 364–369.

918 Ichihara K, Fukubayashi Y (2010) Preparation of fatty acid methyl esters for gas-liquid
919 chromatography. *Journal of Lipid Research* **51**, 635–640.

920 Ishii K, Fujitani H, Sekiguchi Y, Tsuneda S (2020) Physiological and genomic
921 characterization of a new ‘*Candidatus Nitrotoga*’ isolate. *Environmental Microbiology* **22**,
922 2365–2382.

923 Kasprak AH, Sepúlveda J, Price-Waldman R, Williford KH, Schoepfer SD, Haggart JW,
924 Ward PD, Summons RE, Whiteside JH (2015) Episodic photic zone euxinia in the
925 northeastern Panthalassic Ocean during the end-Triassic extinction. *Geology* **43**, 307–310.

926 Katoh K, Standley DM (2013) MAFFT Multiple Sequence Alignment Software Version 7:
927 Improvements in Performance and Usability. *Molecular Biology and Evolution* **30**, 772–780.

928 Kessel MAHJ van, Speth DR, Albertsen M, Nielsen PH, Op den Camp HJM, Kartal B, Jetten
929 MSM, Lücker S (2015) Complete nitrification by a single microorganism. *Nature* **528**, 555–
930 559.

931 Kharbush JJ, Kejriwal K, Aluwihare LI (2015) Distribution and Abundance of Hopanoid
932 Producers in Low-Oxygen Environments of the Eastern Pacific Ocean. *Microbial Ecology*
933 401–408.

934 Kharbush JJ, Thompson LR, Haroon MF, Knight R, Aluwihare LI (2018) Hopanoid-
935 producing bacteria in the Red Sea include the major marine nitrite oxidizers. *FEMS*
936 *Microbiology Ecology* **94**.

937 Kharbush JJ, Ugalde JA, Hogle SL, Allen EE, Aluwihare LI (2013) Composite bacterial
938 hopanoids and their microbial producers across oxygen gradients in the water column of the
939 California current. *Applied and Environmental Microbiology* **79**, 7491–7501.

940 Kitzing K, Koch H, Lückner S, Sedlacek CJ, Herbold C, Schwarz J, Daebeler A, Mueller AJ,
941 Lukumbuzya M, Romano S, Leisch N, Karst SM, Kirkegaard R, Albertsen M, Nielsen PH,
942 Wagner M, Daims H (2018) Characterization of the First “ Candidatus Nitrotoga” Isolate
943 Reveals Metabolic Versatility and Separate Evolution of Widespread Nitrite-Oxidizing
944 Bacteria. *mBio* **9**.

945 Koops H-P, Pommerening-Röser A (2015) The Lithoautotrophic Ammonia-Oxidizing
946 Bacteria. In: *Bergey’s Manual of Systematics of Archaea and Bacteria*. American Cancer
947 Society, pp. 1–17.

948 Koops H-P, Purkhold U, Pommerening-Röser A, Timmermann G, Wagner M (2006) The
949 Lithoautotrophic Ammonia-Oxidizing Bacteria. In: *The Prokaryotes* (eds. Dworkin M,
950 Falkow S, Rosenberg E, Schleifer K-H, Stackebrandt E). Springer New York, New York,
951 NY, pp. 778–811.

952 Kuypers MMM (2001) Massive Expansion of Marine Archaea During a Mid-Cretaceous
953 Oceanic Anoxic Event. *Science* **293**, 92–95.

954 Kuypers MMM, Blokker P, Hopmans EC, Kinkel H, Pancost RD, Schouten S, Sinninghe
955 Damsté JS (2002) Archaeal remains dominate marine organic matter from the early Albian
956 oceanic anoxic event 1b. *Palaeogeography, Palaeoclimatology, Palaeoecology* **185**, 211–
957 234.

958 Kuypers MMM, Breugel Y van, Schouten S, Erba E, Sinninghe Damsté JS (2004) N₂-fixing
959 cyanobacteria supplied nutrient N for Cretaceous oceanic anoxic events. *Geology* **32**, 853.

960 Lengger SK, Rush D, Mayser JP, Blewett J, Schwartz-Narbonne R, Talbot HM, Middelburg
961 JJ, Jetten MSM, Schouten S, Damsté JSS, Pancost RD (2019) Dark carbon fixation in the
962 Arabian Sea oxygen minimum zone contributes to sedimentary organic carbon (SOM).
963 *Global Biogeochemical Cycles* **33**, 1715–1732.

964 Letunic I, Bork P (2016) Interactive tree of life (iTOL) v3: an online tool for the display and
965 annotation of phylogenetic and other trees. *Nucleic Acids Research* **44**, W242–W245.

966 Liu W, Sakr E, Schaeffer P, Talbot HM, Donisi J, Härtner T, Kannenberg E, Takano E,
967 Rohmer M (2014) Ribosylhopane, a Novel Bacterial Hopanoid, as Precursor of C₃₅
968 Bacteriohopanepolyols in *Streptomyces coelicolor* A3(2). *ChemBioChem* **15**, 2156–2161.

969 Lückner S, Nowka B, Rattei T, Spieck E, Daims H (2013) The Genome of *Nitrospina gracilis*
970 Illuminates the Metabolism and Evolution of the Major Marine Nitrite Oxidizer. *Frontiers in*
971 *Microbiology* **4**.

972 Lückner S, Wagner M, Maixner F, Pelletier E, Koch H, Vacherie B, Rattei T, Damsté JSS,
973 Spieck E, Paslier D Le, Daims H (2010) A *Nitrospira* metagenome illuminates the
974 physiology and evolution of globally important nitrite-oxidizing bacteria. *Proceedings of the*
975 *National Academy of Sciences of the United States of America* **107**, 13479–13484.

976 Lunau M, Lemke A, Walther K, Martens-Habbena W, Simon M (2005) An improved method
977 for counting bacteria from sediments and turbid environments by epifluorescence
978 microscopy. *Environmental Microbiology* **7**, 961–968.

979 Mangiarotti A, Genovese DM, Naumann CA, Monti MR, Wilke N (2019) Hopanoids, like
980 sterols, modulate dynamics, compaction, phase segregation and permeability of membranes.
981 *Biochimica et Biophysica Acta (BBA) - Biomembranes* **1861**, 183060.

982 Matys ED, Sepúlveda J, Pantoja S, Lange CB, Caniupán M, Lamy F, Summons RE (2017)
983 Bacteriohopanepolyols along redox gradients in the Humboldt Current System off northern
984 Chile. *Geobiology* **15**, 844–857.

985 McNevin DB, Badger MR, Whitney SM, Caemmerer S von, Tcherkez GGB, Farquhar GD
986 (2007) Differences in Carbon Isotope Discrimination of Three Variants of D-Ribulose-1,5-
987 biphosphate Carboxylase/Oxygenase Reflect Differences in Their Catalytic Mechanisms.
988 *Journal of Biological Chemistry* **282**, 36068–36076.

989 Meer MTJ van der, Schouten S, Sinninghe Damsté JS (1998) The effect of the reversed
990 tricarboxylic acid cycle on the ¹³C contents of bacterial lipids. *Geochimica et Cosmochimica*
991 *Acta* **28**, 527–533.

992 Menzel D, Hopmans EC, Schouten S, Sinninghe Damsté JS (2006) Membrane tetraether
993 lipids of planktonic Crenarchaeota in Pliocene sapropels of the eastern Mediterranean Sea.
994 *Palaeogeography, Palaeoclimatology, Palaeoecology* **239**, 1–15.

995 Mincer TJ, Church MJ, Taylor LT, Preston C, Karl DM, DeLong EF (2007) Quantitative
996 distribution of presumptive archaeal and bacterial nitrifiers in Monterey Bay and the North
997 Pacific Subtropical Gyre. *Environmental Microbiology* **9**, 1162–1175.

998 Mueller AJ, Jung M-Y, Strachan CR, Herbold CW, Kirkegaard RH, Wagner M, Daims H
999 (2020) Genomic and kinetic analysis of novel Nitrospinae enriched by cell sorting. *The ISME*
1000 *Journal* 1–14.

1001 Naafs BDA, Monteiro FM, Pearson A, Higgins MB, Pancost RD, Ridgwell A (2019)
1002 Fundamentally different global marine nitrogen cycling in response to severe ocean
1003 deoxygenation. *Proceedings of the National Academy of Sciences* **116**, 24979–24984.

1004 Newman DK, Neubauer C, Ricci JN, Wu C-H, Pearson A (2016) Cellular and Molecular
1005 Biological Approaches to Interpreting Ancient Biomarkers. *Annual Review of Earth and*
1006 *Planetary Sciences* **44**, 493–522.

1007 Ourisson G, Albrecht P (1992) Hopanoids. 1. Geohopanoids: The Most Abundant Natural
1008 Products on Earth? *Accounts of Chemical Research* **25**, 398–402.

1009 Ourisson G, Rohmer M (1992) Hopanoids. 2. Biohopanoids: A Novel Class of Bacterial
1010 Lipids. *Accounts of Chemical Research* **25**, 403–408.

1011 Ourisson G, Rohmer M, Poralla K (1987) Prokaryotic Hopanoids and other Polyterpenoid
1012 Sterol Surrogates. *Annual Review of Microbiology* **41**, 301–333.

1013 Pachiadaki MG, Sintès E, Bergauer K, Brown JM, Record NR, Swan BK, Mathyer ME,
1014 Hallam SJ, Lopez-Garcia P, Takaki Y, Nunoura T, Woyke T, Herndl GJ, Stepanauskas R
1015 (2017) Major role of nitrite-oxidizing bacteria in dark ocean carbon fixation. *Science* **358**,
1016 1046–1051.

1017 Palomo A, Pedersen AG, Fowler SJ, Dechesne A, Sicheritz-Pontén T, Smets BF (2018)
1018 Comparative genomics sheds light on niche differentiation and the evolutionary history of
1019 comammox *Nitrospira*. *The ISME Journal* **12**, 1779.

1020 Pearson A, Flood Page SR, Jorgenson TL, Fischer WW, Higgins MB (2007) Novel hopanoid
1021 cyclases from the environment. *Environmental Microbiology* **9**, 2175–2188.

1022 Picone N, Pol A, Mesman R, Kessel MAHJ van, Cremers G, Gelder AH van, Alen TA van,
1023 Jetten MSM, Lückner S, Op den Camp HJM (2020) Ammonia oxidation at pH 2.5 by a new
1024 gammaproteobacterial ammonia-oxidizing bacterium. *The ISME Journal* 1–15.

1025 Poger D, Mark AE (2013) The Relative Effect of Sterols and Hopanoids on Lipid Bilayers:
1026 When Comparable Is Not Identical. *The Journal of Physical Chemistry B* **117**, 16129–16140.

1027 Polik CA, Elling FJ, Pearson A (2018) Impacts of Paleoecology on the TEX₈₆ Sea Surface
1028 Temperature Proxy in the Pliocene-Pleistocene Mediterranean Sea. *Paleoceanography and*
1029 *Paleoclimatology* **33**, 1472–1489.

1030 Preuß A, Schauder R, Fuchs G, Stichler W (1989) Carbon isotope fractionation by
1031 autotrophic bacteria with three different CO₂ fixation pathways. *Zeitschrift für*
1032 *Naturforschung* **44**, 397–402.

1033 Quandt L, Gottschalk G, Ziegler H, Stichler W (1977) Isotope discrimination by
1034 photosynthetic bacteria. *FEMS Microbiology Letters* **1**, 125–128.

1035 Quast C, Pruesse E, Yilmaz P, Gerken J, Schweer T, Yarza P, Peplies J, Glöckner FO (2013)
1036 The SILVA ribosomal RNA gene database project: improved data processing and web-based
1037 tools. *Nucleic Acids Research* **41**, D590–D596.

1038 Rashby SE, Sessions AL, Summons RE, Newman DK (2007) Biosynthesis of 2-
1039 methylbacteriohopanepolyols by an anoxygenic phototroph. *Proceedings of the National*
1040 *Academy of Sciences* **104**, 15099–15104.

1041 Ricci JN, Coleman ML, Welander P V, Sessions AL, Summons RE, Spear JR, Newman DK
1042 (2013) Diverse capacity for 2-methylhopanoid production correlates with a specific
1043 ecological niche. *The ISME journal* **8**, 1–10.

1044 Ricci JN, Coleman ML, Welander P V, Sessions AL, Summons RE, Spear JR, Newman DK
1045 (2014) Diverse capacity for 2-methylhopanoid production correlates with a specific
1046 ecological niche. *The ISME Journal* **8**, 675–684.

1047 Ricci JN, Michel AJ, Newman DK (2015) Phylogenetic analysis of HpnP reveals the origin
1048 of 2-methylhopanoid production in Alphaproteobacteria. *Geobiology* **13**, 267–277.

1049 Richardson TL, Jackson GA (2007) Small Phytoplankton and Carbon Export from the
1050 Surface Ocean. *Science* **315**, 838–840.

1051 Rohmer M, Bouvier-Nave P, Ourisson G (1984) Distribution of Hopanoid Triterpenes in
1052 Prokaryotes. *Microbiology* **130**, 1137–1150.

1053 Rush D, Osborne KA, Birgel D, Kappler A, Hirayama H, Peckmann J, Poulton SW, Nickel
1054 JC, Mangelsdorf K, Kalyuzhnaya M, Sidgwick FR, Talbot HM (2016) The
1055 bacteriohopanepolyol inventory of novel aerobic methane oxidising bacteria reveals new
1056 biomarker signatures of aerobic methanotrophy in marine systems. *PLoS ONE* **11**, 1–27.

1057 Sáenz JP (2010) Exploring the distribution and physiological roles of bacterial membrane
1058 lipids in the marine environment (PhD Thesis).

1059 Sáenz JP, Sezgin E, Schwille P, Simons K (2012) Functional convergence of hopanoids and
1060 sterols in membrane ordering. *Proceedings of the National Academy of Sciences* **109**, 14236–
1061 14240.

1062 Sáenz JP, Wakeham SG, Eglinton TI, Summons RE (2011) New constraints on the
1063 provenance of hopanoids in the marine geologic record: Bacteriohopanepolyols in marine
1064 suboxic and anoxic environments. *Organic Geochemistry* **42**, 1351–1362.

1065 Sakata S, Hayes JM, Rohmer M, Hooper AB, Seemann M (2008) Stable carbon-isotopic
1066 compositions of lipids isolated from the ammonia-oxidizing chemoautotroph *Nitrosomonas*
1067 *europaea*. *Organic Geochemistry, Stable Isotopes in Biogeosciences (II)* **39**, 1725–1734.

1068 Santoro AE, Casciotti KL, Francis CA (2010) Activity, abundance and diversity of nitrifying
1069 archaea and bacteria in the central California Current. *Environmental Microbiology* **12**,
1070 1989–2006.

1071 Sato S, Kudo F, Rohmer M, Eguchi T (2020) Characterization of Radical SAM
1072 Adenosylhopane Synthase, HpnH, which Catalyzes the 5'-Deoxyadenosyl Radical Addition
1073 to Diploptene in the Biosynthesis of C₃₅ Bacteriohopanepolyols. *Angewandte Chemie*
1074 *International Edition* **59**, 237–241.

1075 Schmerk CL, Welander PV, Hamad MA, Bain KL, Bernards MA, Summons RE, Valvano
1076 MA (2015) Elucidation of the *Burkholderia cenocepacia* hopanoid biosynthesis pathway
1077 uncovers functions for conserved proteins in hopanoid-producing bacteria. *Environmental*
1078 *Microbiology* **17**, 735–750.

1079 Schopfer FJ, Khoo NKH (2019) Nitro-Fatty Acid Logistics: Formation, Biodistribution,
1080 Signaling, and Pharmacology. *Trends in Endocrinology & Metabolism* **30**, 505–519.

1081 Seemann M, Bisseret P, Tritz J-P, Hooper AB, Rohmer M (1999) Novel bacterial
1082 triterpenoids of the hopane series from *Nitrosomonas europaea* and their significance for the
1083 formation of the C₃₅ bacteriohopane skeleton. *Tetrahedron Letters* **40**, 1681–1684.

1084 Sinninghe Damsté JS, Rijpstra WIC, Dedysh SN, Foesel BU, Villanueva L (2017) Pheno-
1085 and Genotyping of Hopanoid Production in Acidobacteria. *Frontiers in Microbiology* **8**.

1086 Sirevåg R, Buchanan BB, Berry JA, Troughton JH (1977) Mechanisms of CO₂ Fixation in
1087 Bacterial Photosynthesis Studied by the Carbon Isotope Fractionation Technique. *Arch.*
1088 *Microbiol.* **112**, 35–38.

1089 Sohlenkamp C, Geiger O (2016) Bacterial membrane lipids: diversity in structures and
1090 pathways. *FEMS Microbiology Reviews* **40**, 133–159.

1091 Sorokin DY, Lückner S, Vejmekova D, Kostrikina NA, Kleerebezem R, Rijpstra WIC,
1092 Damsté JSS, Paslier D Le, Muyzer G, Wagner M, Loosdrecht MCM van, Daims H (2012)
1093 Nitrification expanded: discovery, physiology and genomics of a nitrite-oxidizing bacterium
1094 from the phylum Chloroflexi. *The ISME Journal* **6**, 2245–2256.

1095 Spencer-Jones CL (2015) Novel Concepts Derived From Microbial Biomarkers In The
1096 Congo System: Implications For Continental Methane Cycling (PhD Thesis).

1097 Spieck E, Bock E (2005) The Lithoautotrophic Nitrite-Oxidizing Bacteria. In: *Bergey's*
1098 *Manual of Systematics of Archaea and Bacteria* (eds. Whitman WB, Rainey F, Kämpfer P,
1099 Trujillo M, Chun J, DeVos P, Hedlund B, Dedysh S). John Wiley & Sons, Ltd, Chichester,
1100 UK, pp. 1–10.

1101 Spieck E, Lipski A (2011) Cultivation, Growth Physiology, and Chemotaxonomy of Nitrite-
1102 Oxidizing Bacteria. In: *Research on Nitrification and Related Processes, Part A, Methods in*
1103 *Enzymology* (ed. Klotz MG). Elsevier, pp. 109–130.

1104 Spieck E, Sass K, Keuter S, Hirschmann S, Spohn M, Indenbirken D, Kop LFM, Lückner S,
1105 Giaveno A (2020a) Defining Culture Conditions for the Hidden Nitrite-Oxidizing Bacterium
1106 Nitrolancea. *Frontiers in Microbiology* **11**.

1107 Spieck E, Spohn M, Wendt K, Bock E, Shively J, Frank J, Indenbirken D, Alawi M, Lückner
1108 S, Hüpeden J (2020b) Extremophilic nitrite-oxidizing Chloroflexi from Yellowstone hot
1109 springs. *The ISME Journal* **14**, 364–379.

1110 Stamatakis A (2014) RAxML version 8: a tool for phylogenetic analysis and post-analysis of
1111 large phylogenies. *Bioinformatics* **30**, 1312–1313.

1112 Strickland JDH, Parsons TR (1972) Ammonium and Nitrite. In: *A practical Handbook of*
1113 *Seawater Analysis*. Fisheries Research Board of Canada, Ottawa.

1114 Sturt HF, Summons RE, Smith K, Elvert M, Hinrichs K-U (2004) Intact polar membrane
1115 lipids in prokaryotes and sediments deciphered by high-performance liquid
1116 chromatography/electrospray ionization multistage mass spectrometry - new biomarkers for
1117 biogeochemistry and microbial ecology. *Rapid Communications in Mass Spectrometry* **18**,
1118 617–628.

1119 Summons RE, Jahnke LL, Hope JM, Logan GA (1999) 2-Methylhopanoids as biomarkers for
1120 cyanobacterial oxygenic photosynthesis. *Nature* **400**, 554–557.

1121 Talbot HM, Bischoff J, Inglis GN, Collinson ME, Pancost RD (2016a) Polyfunctionalised
1122 bio- and geohopanooids in the Eocene Cobham Lignite. *Organic Geochemistry* **96**, 77–92.

1123 Talbot HM, Handley L, Spencer-Jones CL, Dinga BJ, Schefuß E, Mann PJ, Poulsen JR,
1124 Spencer RGM, Wabakanghanzi JN, Wagner T (2014) Variability in aerobic methane
1125 oxidation over the past 1.2 Myrs recorded in microbial biomarker signatures from Congo fan
1126 sediments. *Geochimica et Cosmochimica Acta* **133**, 387–401.

- 1127 Talbot HM, McClymont EL, Inglis GN, Evershed RP, Pancost RD (2016b) Origin and
1128 preservation of bacteriohopanepolyol signatures in Sphagnum peat from Bissendorfer Moor
1129 (Germany). *Organic Geochemistry* **97**, 95–110.
- 1130 Talbot HM, Rohmer M, Farrimond P (2007) Structural characterisation of unsaturated
1131 bacterial hopanoids by atmospheric pressure chemical ionisation liquid chromatography/ion
1132 trap mass spectrometry. *Rapid Communications in Mass Spectrometry* **21**, 1613–1622.
- 1133 Talbot HM, Summons RE, Jahnke LL, Cockell CS, Rohmer M, Farrimond P (2008)
1134 Cyanobacterial bacteriohopanepolyol signatures from cultures and natural environmental
1135 settings. *Organic Geochemistry* **39**, 232–263.
- 1136 Tang T, Mohr W, Sattin SR, Rogers DR, Girguis PR, Pearson A (2017) Geochemically
1137 distinct carbon isotope distributions in *Allochrochromatium vinosum* DSM 180^T grown
1138 photoautotrophically and photoheterotrophically. *Geobiology* **15**, 324–339.
- 1139 Thiel V, Blumenberg M, Pape T, Seifert R, Michaelis W (2003) Unexpected occurrence of
1140 hopanoids at gas seeps in the Black Sea. *Organic Geochemistry* **34**, 81–87.
- 1141 Tyrrell T (1999) The relative influences of nitrogen and phosphorus on oceanic primary
1142 production. *Nature* **400**, 525–531.
- 1143 Van Cappellen P, Ingall ED (1996) Redox Stabilization of the Atmosphere and Oceans by
1144 Phosphorus-Limited Marine Productivity. *Science* **271**, 493–496.
- 1145 Wakeham SG, Amann R, Freeman KH, Hopmans EC, Jørgensen BB, Putnam IF, Schouten S,
1146 Sinninghe Damsté JS, Talbot HM, Woebken D (2007) Microbial ecology of the stratified
1147 water column of the Black Sea as revealed by a comprehensive biomarker study. *Organic*
1148 *Geochemistry* **38**, 2070–2097.
- 1149 Wakeham SG, Turich C, Schubotz F, Podlaska A, Li XN, Varela R, Astor Y, Sáenz JP, Rush
1150 D, Sinninghe Damsté JS, Summons RE, Scranton MI, Taylor GT, Hinrichs K-U (2012)
1151 Biomarkers, chemistry and microbiology show chemoautotrophy in a multilayer chemocline
1152 in the Cariaco Basin. *Deep Sea Research Part I: Oceanographic Research Papers* **63**, 133–
1153 156.
- 1154 Ward BB, Carlucci AF (1985) Marine Ammonia- and Nitrite-Oxidizing Bacteria: Serological
1155 Diversity Determined by Immunofluorescence in Culture and in the Environment. *Applied*
1156 *and Environmental Microbiology* **50**, 8.
- 1157 Ward BB, Glover HE, Lipschultz F (1989) Chemoautotrophic activity and nitrification in the
1158 oxygen minimum zone off Peru. *Deep Sea Research Part A. Oceanographic Research*
1159 *Papers* **36**, 1031–1051.

- 1160 Warren MJ, Raux E, Schubert HL, Escalante-Semerena JC (2002) The biosynthesis of
1161 adenosylcobalamin (vitamin B₁₂). *Natural Product Reports* **19**, 390–412.
- 1162 Watson SW, Waterbury JB (1971) Characteristics of two marine nitrite oxidizing bacteria,
1163 *Nitrospina gracilis* nov. gen. nov. sp. and *Nitrococcus mobilis* nov. gen. nov. sp. *Archiv für*
1164 *Mikrobiologie* **77**, 203–230.
- 1165 Welander P V, Coleman ML, Sessions AL, Summons RE, Newman DK (2010) Identification
1166 of a methylase required for 2-methylhopanoid production and implications for the
1167 interpretation of sedimentary hopanes. *Proceedings of the National Academy of Sciences of*
1168 *the United States of America* **107**, 8537–42.
- 1169 Welander P V, Summons RE (2012) Discovery, taxonomic distribution, and phenotypic
1170 characterization of a gene required for 3-methylhopanoid production. *Proceedings of the*
1171 *National Academy of Sciences of the United States of America* **109**, 12905–12910.
- 1172 Welander PV, Doughty DM, Wu C-H, Mehay S, Summons RE, Newman DK (2012)
1173 Identification and characterization of *Rhodopseudomonas palustris* TIE-1 hopanoid
1174 biosynthesis mutants. *Geobiology* **10**, 163–177.
- 1175 Welander PV, Hunter RC, Zhang L, Sessions AL, Summons RE, Newman DK (2009)
1176 Hopanoids Play a Role in Membrane Integrity and pH Homeostasis in *Rhodopseudomonas*
1177 *palustris* TIE-1. *Journal of Bacteriology* **191**, 6145–6156.
- 1178 Williams TJ, Zhang CL, Scott JH, Bazylinski DA (2006) Evidence for Autotrophy via the
1179 Reverse Tricarboxylic Acid Cycle in the Marine Magnetotactic Coccus Strain MC-1. *Applied*
1180 *and Environmental Microbiology* **72**, 1322–1329.
- 1181 Wu C-H, Bialecka-Fornal M, Newman DK (2015) Methylation at the C-2 position of
1182 hopanoids increases rigidity in native bacterial membranes. *eLife* **4**, e05663.
- 1183 Zhu C, Talbot HM, Wagner T, Pan J-M, Pancost RD (2011) Distribution of hopanoids along
1184 a land to sea transect: Implications for microbial ecology and the use of hopanoids in
1185 environmental studies. *Limnology and Oceanography* **56**, 1850–1865.

1186

1187

1188 **Figure captions**

1189 **Fig. 1.** Pathways and mediating enzymes (blue) of bacteriohopanepolyol biosynthesis
1190 and structural modification (after Welander et al., 2010; Bradley et al., 2010; Welander et al.,
1191 2012; Liu et al., 2014; Schmerk et al., 2015; Sohlenkamp and Geiger, 2016; Belin et al.,

1192 2018). The order of methylhopanoid biosynthesis and the enzymes responsible for BHT
1193 formation and the pathways leading to other bacteriohopanepolyols (such as
1194 aminobacteriohopanetetrol and aminobacteriohopanepentol) are not known. Note that
1195 methylation at C-2 (HpnP) or C-3 (HpnR) can occur not only in BHT but also in other
1196 hopanoids.

1197 **Fig. 2.** Distribution of hopanoid biosynthetic genes (grey squares: presence of gene;
1198 white squares: absence of gene; see also Table S1) in genomes of selected nitrite-oxidizing
1199 bacteria (pink; NOB), ammonia-oxidizing bacteria (cyan; AOB), complete ammonia-
1200 oxidizers (purple; COMAMMOX), and closely related, non-nitrifying bacteria. Habitat is
1201 indicated by colored circles. For additional data from cultivated nitrifiers and environmental
1202 genomes, see Supplementary Datafile S1. Species analyzed for BHP content in this study are
1203 highlighted in bold. The tree represents the 16S rRNA gene phylogeny of nitrifiers and
1204 closely related organisms, with phyla and proteobacterial classes (α , β , γ , δ) indicated along
1205 the branches. Circles indicate branches with >90% support based on 500 bootstrap analyses.
1206 The scale bar represents 0.1 substitutions per nucleotide.

1207 **Fig. 3.** (A) Composite extracted ion chromatograms of novel BHPs (m/z $[M+H]^+$ 638.5,
1208 656.6, 748.5, 743.6, 762.5, 771.6) and previously characterized BHPs (aminotriol,
1209 aminopentol, bacteriohopanetetrol) from *Nitrobacter vulgaris* and *Nitrococcus mobilis* (factor
1210 indicates magnification of small peaks). (B-G) MS² fragmentation spectra and tentative
1211 structural identification of novel BHPs. Positions of functional groups along the extended
1212 hopanoid backbone are speculative. Note that consecutive losses of -42 (CH₂CO), and -18
1213 (H₂O) can be generated through cleavage of any acetylated hydroxyl group but could also be
1214 generated through cleavage of acetylated nitro groups. Accurate masses and proposed sum
1215 formulas of major fragment ions are shown in Table S4. Interpretation of fragmentation
1216 patterns is provided in the supplementary information.

1217

1218 **Fig. 4.** Relative abundance of hopanoids (averages of triplicate cultures, except for
1219 single cultures for pseudocobalamin) in four freshwater/wastewater species of nitrite-
1220 oxidizing bacteria under varying growth conditions: autotrophic (NO₂⁻ as electron donor;
1221 MG: mid-growth phase, ES: early stationary phase), autotrophic + methionine (ES),
1222 autotrophic + cobalamin (ES), autotrophic + cobalamin + methionine + 6h/18h light/dark
1223 cycles (ES), autotrophic + pseudocobalamin, mixotrophic (NO₂⁻ + complex organics; ES),

1224 heterotrophic aerobic (complex organics but no NO_2^- ; ES), heterotrophic anaerobic (complex
1225 organics but N_2 headspace; ES), NO_2^- -limited chemostat (growth rate 0.013 h^{-1}), O_2 -limited
1226 chemostat (0.013 h^{-1}). Relative abundances of major bacteriohopanepolyols (BHPs) are
1227 shown in panels **A-D** (BHT: bacteriohopanetetrol; BHaminotriol: 35-
1228 aminobacteriohopanetriol; BHaminopentol: aminobacteriohopanepentol). Abundances of
1229 total BHPs relative to 2-methyl BHPs and the non-functionalized hopanoids diploptene and
1230 2-methyl diploptene are shown in panels **E-H** (data for panel H from Elling et al., 2020).
1231 Abundances of total hopanoids (BHPs + 2-methyl BHPs + diploptene + 2-methyl diploptene)
1232 are shown in panels **I-L** (vertical line: average; n.a., not available). Distribution of minor
1233 BHPs (< 2% relative abundance) shown in Table S2.

1234

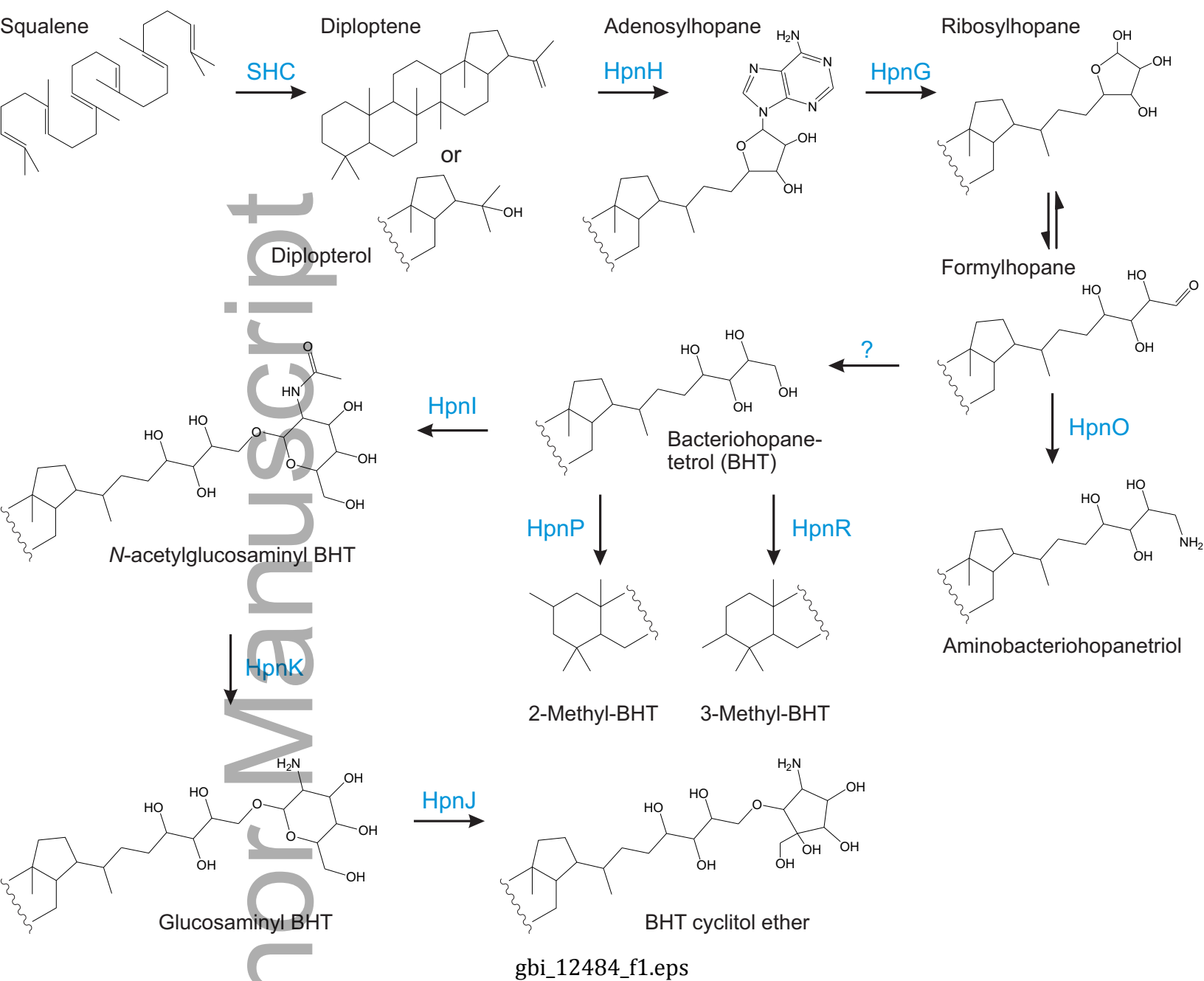
1235 **Fig. 5.** Relative abundance of hopanoids (averages of triplicate cultures, except for
1236 duplicate cultures for *N. mobilis* and *N. gracilis* chemostat experiments, single culture for
1237 pseudocobalamin) in three marine species of nitrite-oxidizing bacteria under varying growth
1238 conditions: autotrophic (NO_2^- as electron donor; ES: early stationary phase, LS: late
1239 stationary phase), autotrophic + methionine (ES), autotrophic + cobalamin (ES), mixotrophic
1240 (NO_2^- + complex organics; ES), autotrophic + pseudocobalamin, NO_2^- -limited chemostat
1241 (growth rate 0.011 h^{-1}), O_2 -limited chemostat (0.011 h^{-1}). Relative abundances of major
1242 bacteriohopanepolyols (BHPs) are shown in panels **A-C** (BHT: bacteriohopanetetrol;
1243 BHaminotriol: 35-aminobacteriohopanetriol). Abundances of total BHPs relative to the non-
1244 functionalized hopanoids diploptene and 2-methyl diploptene are shown in panels **D-F**.
1245 Abundances of total hopanoids (BHPs + diploptene) are shown in panels **G-I** (vertical line:
1246 average). Distribution of minor BHPs (< 2% relative abundance) shown in Table S2. Please
1247 note that 2-methyl derivatives of BHT, BHPs, and diploptene were not detected in any of the
1248 strains shown.

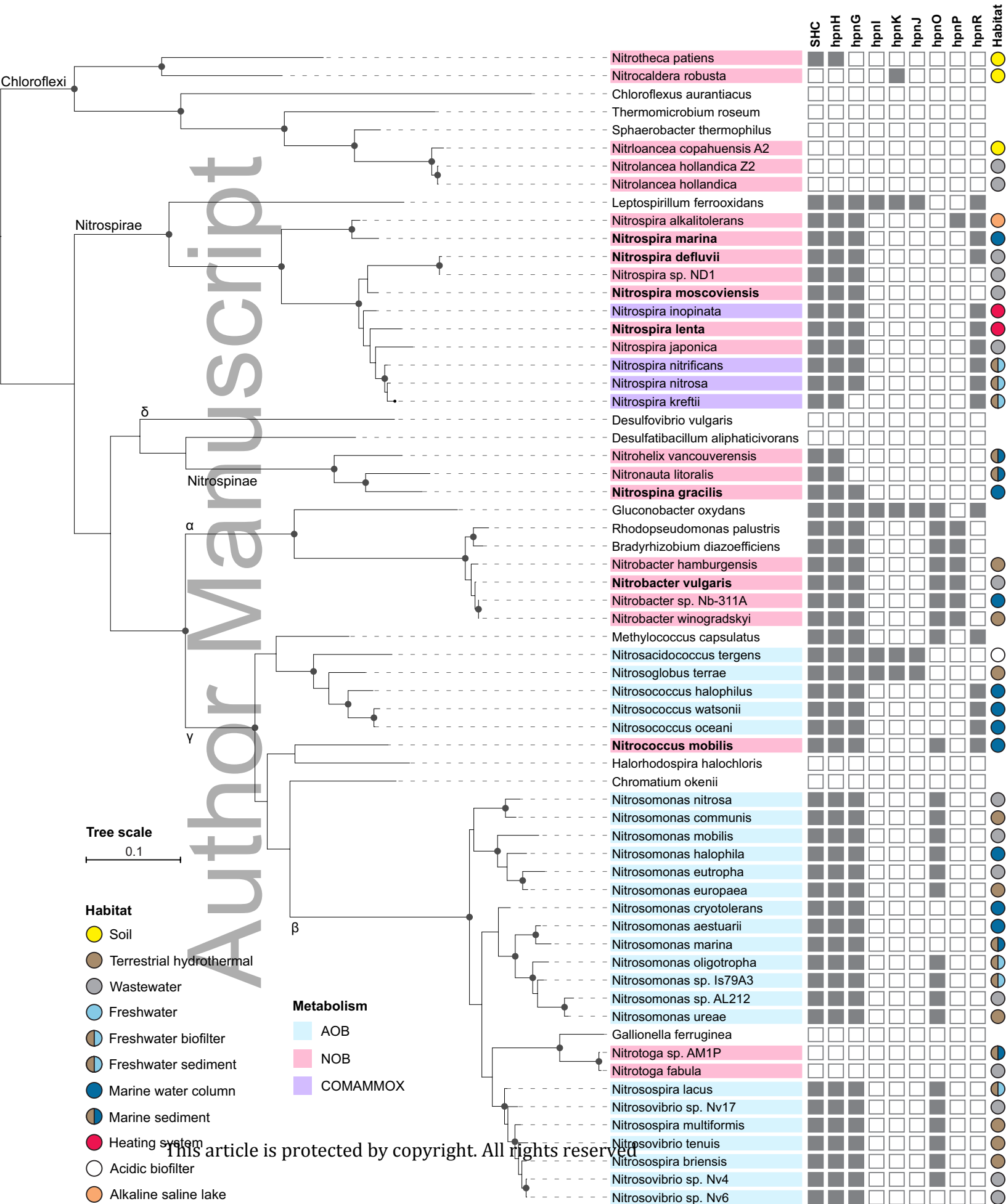
Table 1. Growth conditions of cultures used in this study (medium type: AFW, artificial freshwater; ASW, artificial seawater; NSW, natural seawater).

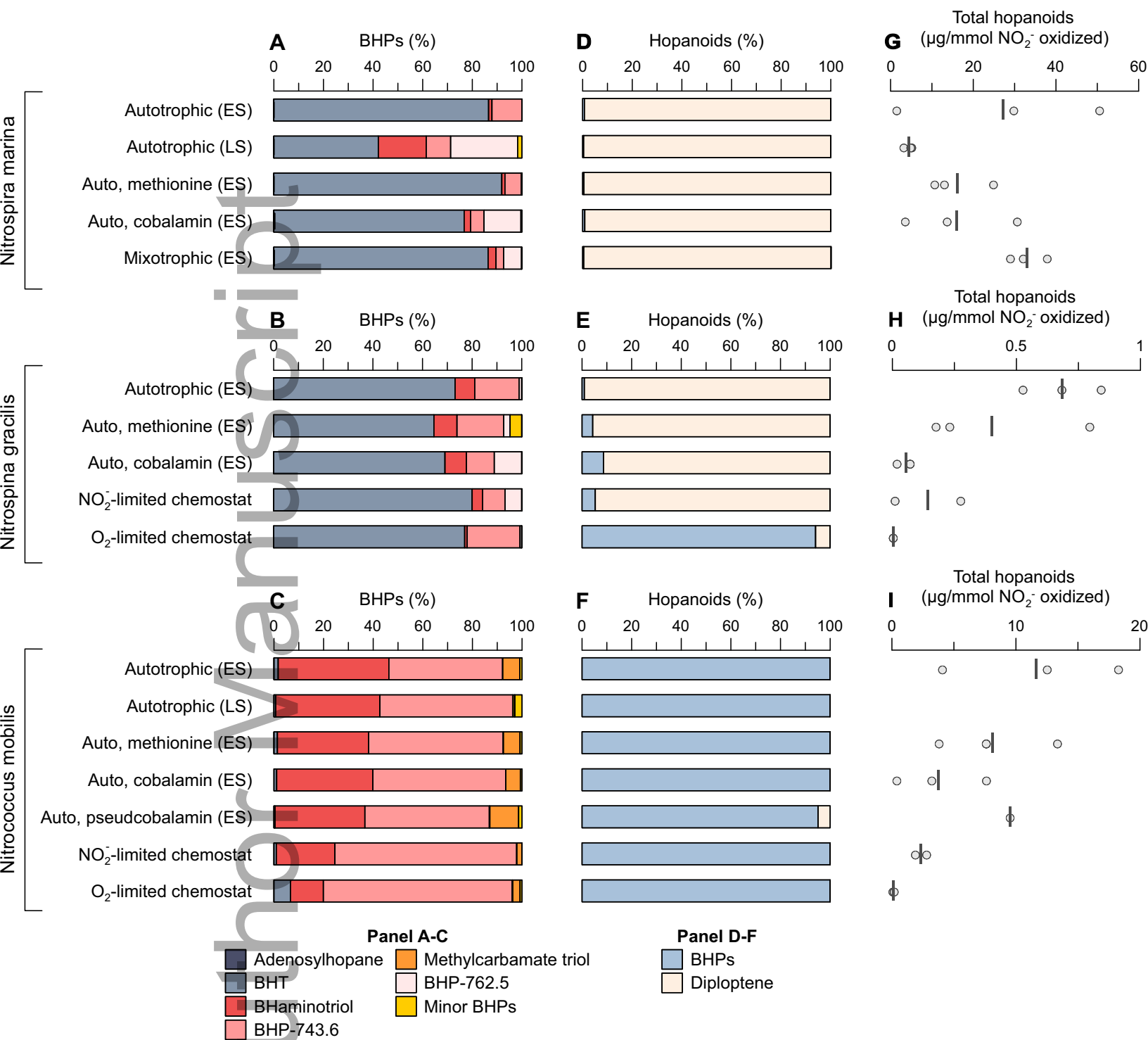
	Medium type	Autotrophic, mid growth	Autotrophic, early stationary	Autotrophic, late stationary	Autotrophic + methionine	Autotrophic + cobalamin	Autotrophic + methionine + cobalamin + light	Mixotrophic	Heterotrophic aerobic	Heterotrophic anaerobic	Nitrite-limited chemostat + methionine + cobalamin	O ₂ -limited chemostat + methionine + cobalamin
<i>Nitrospina gracilis</i> Nb-3/211	NSW		✓		✓	✓						
<i>Nitrospina gracilis</i> Nb-211	ASW										✓	✓
<i>Nitrospira marina</i> Nb-295	NSW		✓	✓	✓	✓		✓				
<i>Nitrococcus mobilis</i> Nb-231	NSW		✓	✓	✓	✓						
<i>Nitrococcus mobilis</i> Nb-231	ASW										✓	✓
<i>Nitrobacter vulgaris</i> AB1	AFW	✓	✓		✓	✓	✓	✓	✓	✓	✓	✓
<i>Nitrospira defluvii</i> A17	AFW		✓									
<i>Nitrospira lenta</i> BS10	AFW		✓									
<i>Nitrospira moscoviensis</i> M-1	AFW		✓									

Table 2. Stable carbon isotopic composition ($\delta^{13}\text{C}$) and carbon isotopic fractionation (ϵ) of dissolved inorganic carbon (DIC), CO_2 (calculated from DIC after Mook et al. (1974), at 28 °C), biomass (bio), summed C_{16} fatty acids (FA; *Nitrospina gracilis*: $\text{C}_{16\omega 9}$; *Nitrospira marina*: $\text{C}_{16:0}+\text{C}_{16:1\omega 5}+\text{C}_{16:1\omega 9}$; *Nitrococcus mobilis*: $\text{C}_{16:0}+\text{C}_{16:1\omega 9}$), summed C_{18} fatty acids (*Nitrococcus mobilis*: $\text{C}_{18:0}+\text{C}_{18\omega 7}$, *Nitrobacter vulgaris*: $\text{C}_{18:0}+\text{C}_{18\omega 1}$), and the hopanoid diploptene in four species chemolithoautotrophically grown nitrite-oxidizing bacteria. Data for *N. vulgaris* are from Elling et al. (2020).

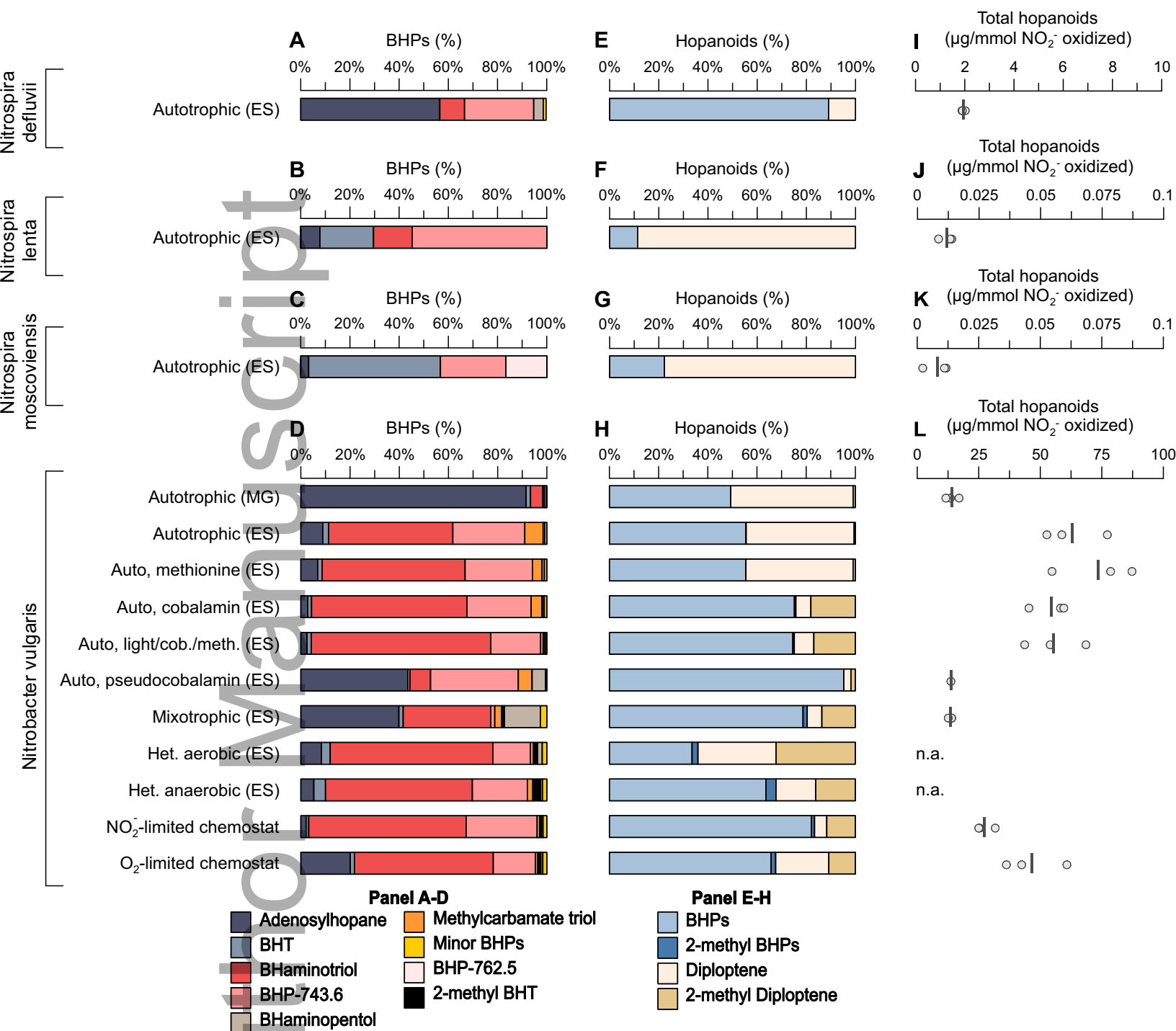
		$\delta^{13}\text{C}_{\text{DIC}}$ (‰)	$\delta^{13}\text{C}_{\text{CO}_2}$ (‰)	$\delta^{13}\text{C}_{\text{bio}}$ (‰)	$\delta^{13}\text{C}_{\text{C16FA}}$ (‰)	$\delta^{13}\text{C}_{\text{C18FA}}$ (‰)	$\delta^{13}\text{C}_{\text{diplop.}}$ (‰)
$\delta^{13}\text{C}$	<i>N. gracilis</i>	-0.5 ± 0.2	-8.9 ± 0.2	-10.9 ± 0.2	-8.5 ± 0.2	-	-16.1 ± 0.9
	<i>N. marina</i>	2.1 ± 0.1	-6.5 ± 0.1	-8.3 ± 0.1	-3.0 ± 0.4	-	-13.5 ± 0.1
	<i>N. mobilis</i>	1.7 ± 0.1	-6.7 ± 0.1	-15.1 ± 0.3	-22.9 ± 0.1	-20.2 ± 0.6	-18.2 ± 1.7
	<i>N. vulgaris</i>	-5.6 ± 0.2	-14 ± 0.2	-36.4 ± 0.2	-	-42.8 ± 0.2	-44.5 ± 0.3
ϵ				$\epsilon_{\text{CO}_2\text{-bio}}$ (‰)	$\epsilon_{\text{CO}_2\text{-C16FA}}$ (‰)	$\epsilon_{\text{CO}_2\text{-C18FA}}$ (‰)	$\epsilon_{\text{CO}_2\text{-diplop.}}$ (‰)
	Relative						
	to substrate						
ϵ					$\epsilon_{\text{bio-C16FA}}$ (‰)	$\epsilon_{\text{bio-C18FA}}$ (‰)	$\epsilon_{\text{bio-diplop.}}$ (‰)
	Relative						
	to biomass						







gbi_12484_f4.eps



gbi_12484_f5.eps